Electronic Supplementary Information (ESI)

Deep insight of reasons for mechanoluminescence phenomenon of triphenylamine-substituted imidazoles and their distinct mechanofluorochromic behaviours

Xiao-Jing Liu, Guan-Lei Gao, Hao Jiang, Yan-Rong Jia, Min Xia*

(Department of Chemistry, Zhejiang Sci-Tech University, Hangzhou 310018, P. R. China)

E-mail: xiamin@zstu.edu.cn

Materials and instruments

All the reagents are analytically pure and some chemicals are further purified by recrystallization or distillation. Melting points re determined by an OptiMelt automatic melting point system. The ^{1}H NMR (400 MHz) and ^{13}C NMR (100 MHz) spectra are obtained on a Bruker Avance II DMX 400 spectrometer with $CDCl_3$ as the solvent. The absorption spectra are measured on a Shimadzu UV 3600 UV-Vis-NIR spectrometer, and the fluorescence spectra are acquired on a Perkin-Elmer LS55 spectrophotometer. The quantum yields are measured with quinine sulfate in 0.1 M sulfuric acid solution (Φ_f =0.55) as the reference. The crystallographic data are determined on a Bruker Gemini Ultra diffractometer with a CCD counter. The powder X-ray diffraction patterns are recorded on DX2700 with Cu-K_α radiation operating at 40 kV and 40 mA by a 0.3°/min scanning rate. ESI-HRMS is measured on a Brucker Daltonics APEXIII spectrometer. The emission decay spectra of as-prepared and ground samples are respectively recorded on FluoroMax-4 and PicoQuant PicoHarp 300 spectrometers.

Synthesis of BIMTPA

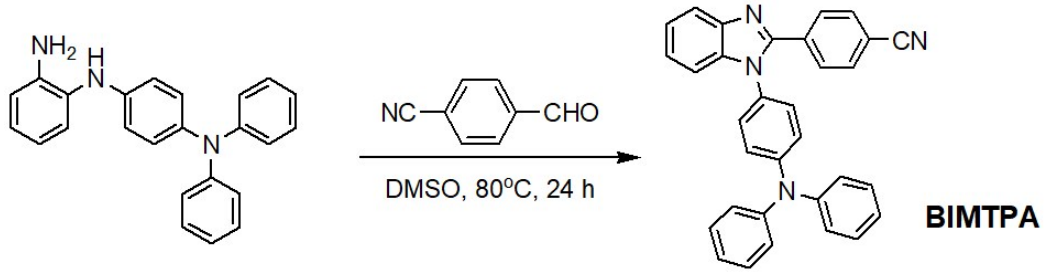

At room temperature, 4-formylbenzonitrile (10 mmol) and N^1-(2-aminophenyl)-N^4,N^4-diphenylbenzene-1,4-diamine (12 mmol) are added into DMSO (30 mL) in an open vessel. The resulted solution is heated at 80 °C for 24 h by using TLC to determine the end of the reaction. After cooling to the room temperature, water (200 mL) is poured into the solution and the mixture is extracted by CH_2Cl_2 (3×20 mL). The combined organic layers are dried over anhydrous Na_2SO_4 and filtrated. The filtrate is concentrated on a rotating evaporator and the residue is purified by the gel silica column chromatography to provide **BIMTPA**.

4-(1-(4-(diphenylamino)phenyl)-1H-benzo[*d*]imidazol-2-yl)benzonitrile (**BIMTPA**): dark yellow solid, 67% yield; m.p. 202.7-203.9 °C; ^{1}H NMR(400M Hz, $CDCl_3$) δ 7.08-7.12(m, 6H), 7.17(d, *J*=8.0 Hz, 4H), 7.31-7.37(m, 7H), 7.63(d, *J*=8.0 Hz, 2H), 7.78(d, *J*=8.0 Hz, 2H), 7.88(d, *J*=8.0 Hz, 1H); ^{13}C NMR(100M Hz, $CDCl_3$) δ 110.87, 112.91, 118.41, 120.16, 123.46, 124.15, 124.25, 125.40, 127.97, 129.02, 129.69, 129.81, 132.03, 134.47, 137.65, 142.75, 146.92, 148.67, 150.08; FT-IR (KBr) ν (cm^{-1}) 3033, 2225, 1591, 1508, 1488, 1314, 1279, 851, 743, 695; HRMS(ESI) *m/z* Calculated for [$C_{32}H_{22}N_4$ + H]: 463.1923; found for [$C_{32}H_{22}N_4$ + H]: 463.1923.

Synthesis of IMTPA and PHIMTPA

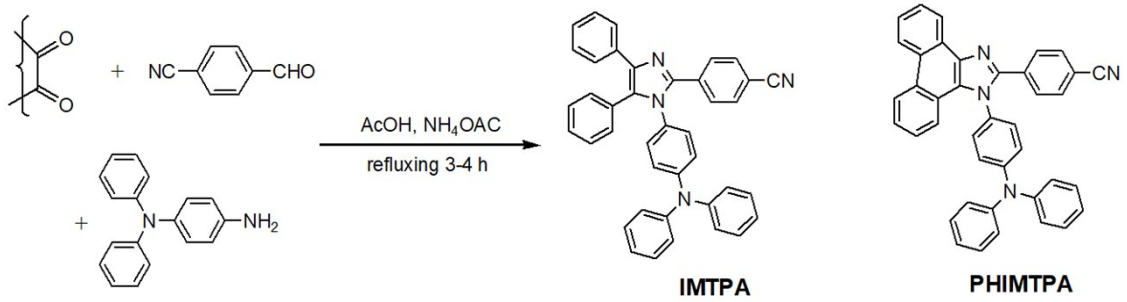

At room temperature, diketone (10 mmol), 4-formylbenzonitrile (10 mmol), N^1,N^1-diphenylbenzene-1,4-diamine (12 mmol) and NH_4OAc (20 mmol) are added into AcOH (20 mL) and the resulting mixture is refluxed for 3-4 h. After cooling, the mixture is poured into water (300 mL) and extracted by $CHCl_3$ (3×20 mL). The combined organic layers are dried over anhydrous Na_2SO_4 and the filtrate is concentrated on a rotating evaporator. The residue is purified by the gel silica column chromatography to provide **IMTPA** or **PHIMTPA**.

4-(1-(4-(diphenylamino)phenyl)-4,5-diphenyl-1H-imidazol-2-yl)benzonitrile (**IMTPA**): bright yellow solid, 78% yield; m.p. 217.9-219.6 °C; ^{1}H NMR(400M Hz, $CDCl_3$) δ 6.83(d, *J*=6.8 Hz, 2H), 6.92(d, *J*=6.8 Hz, 2H), 7.04(d, *J*=7.6 Hz, 4H), 7.08(d, *J*=7.6 Hz, 2H), 7.16(d, *J*=8.0 Hz, 2H), 7.21(d, *J*=8.0 Hz, 1H), 7.24-7.31(m, 9H), 7.58(d, *J*=8.8 Hz, 4H), 7.67(d, *J*=8.8 Hz, 2H); ^{13}C NMR(100M Hz, $CDCl_3$) δ 111.54, 118.75, 122.28, 124.01, 125.10, 126.99, 127.34, 128.28, 128.33, 128.42, 128.93, 128.97, 129.56, 130.17, 131.14, 131.90, 132.43, 133.87, 134.72, 138.86, 144.61, 146.91, 148.35; FT-IR (KBr) ν (cm^{-1}) 3057, 2224, 1591,

1508, 1332, 1289, 850, 774, 756, 698; HRMS(ESI) *m/z* Calculated for [$C_{40}H_{28}N_4$ + H]: 565.2392; found for [$C_{40}H_{28}N_4$ + H]: 565.2394.

4-(1-(4-(diphenylamino)phenyl)-1H-phenanthro[9,10-*d*]imidazol-2-yl)benzonitrile (**PHIMTPA**): 83% yield, white solid; m.p. 240.7-242.6 ^oC; ^1H NMR(400M Hz, $CDCl_3$) δ 7.12-7.25(m, 10H), 7.35-7.41(m, 6H), 7.50-7.56(m, 3H), 7.62(dt, J_1=8.0 Hz, J_2=1.2 Hz, 1H), 7.67-7.73(m, 3H), 8.65(d, *J*=8.4 Hz, 1H), 8.73(d, *J*=8.4 Hz, 1H), 8.80(dd, J_1=8.0 Hz, J_2=1.2 Hz, 1H); ^{13}C NMR(100M Hz, $CDCl_3$) δ 111.98, 118.67, 121.08, 122.54, 122.68, 122.94, 123.23, 124.25, 124.48, 125.45, 125.52, 125.99, 126.47, 127.02, 127.46, 128.45, 128.96, 129.40, 129.47, 129.67, 129.81, 130.68, 131.85, 139.82, 137.53, 146.85, 148.47, 149.51; FT-IR (KBr) ν (cm^{-1}) 3062, 2225, 1590, 1489, 1320, 1287, 845, 755, 698; HRMS(ESI) *m/z* Calculated for [$C_{40}H_{26}N_4$ + H]: 563.2236; found for [$C_{40}H_{26}N_4$ + H]: 563.2241.

X-Ray structure analysis

Single crystals of the title compounds grown in $CHCl_3$/EtOH are selected for the X-ray analysis. The diffraction data are collected on a Bruker CCD area-detector diffractometer equipped with a graphite-monochromated Mo (λ=0.71073Å) or Cu (λ=1.54178 Å) radiation. The unit cell parameters are determined from a least-squares refinement of the setting angles. The structure is solved by direct methods and refined on F^2 by the full-matrix least-squares methods with SHELXS-97. The refinement is carried out by full-matrix least squares method on the positional and anisotropic temperature parameters of the non-hydrogen atoms using SHELXL-97. All H atoms are placed in the idealized positions and constrained to ride on their parent atoms. Crystallographic data for **IMTPA** (CCDC 1959200), **BIMTPA** (CCDC 1959202) and **PHIMTPA** (CCDC 1959204) are deposited at CCDC centre and can be obtained free of charge from The Cambridge Crystallographic Data Centre via www.ccdc.cam.ac.uk/ data_request/cif.

Table S1 Crystallographic data for **IMTPA**, **BIMTPA** and **PHIMTPA**

	IMTPA	**BIMTPA**	**PHIMTPA**
	a = 13.9738(4) Å	*a* = 13.2852(5) Å	*a* = 13.0705(4) Å
	b = 9.4252(2) Å	*b* = 9.7783(3) Å	*b* = 9.7279(3) Å
	c = 22.9485(6) Å	*c* = 18.6415(6) Å	*c* =22.9944(7) Å
	α =90 °	*α* = 90 °	*α* = 90 °
	β =102.300(1) °	*β* = 94.186(1) °	*β* = 101.425(1) °
	γ =90 °	*γ* = 90 °	*γ* = 90 °
Temperature	170 K	170 K	170 K
Wavelength	0.71073 Å	0.71073 Å	1.54178 Å
Volume	2953.07(13)	2415.20(14)	2677.54(19)
Space group	$P_{21/n}$	$P_{21/c}$	$P_{21/n}$
Hall group	P_{2yn}	P_{2ybc}	P_{2yn}
Density	1.270 g/cm^3	1.272 g/cm^3	1.304 g/cm^3
Z	4	4	4
Mu	0.075 / mm	0.076 / mm	0.077 / mm
F_{000}	1184.0	968.0	1176.0
h, k, l (max)	17,11, 29	17,12, 23	16,12, 29
N_{ref}	6266	5301	6322
T_{min}, T_{max}	0.708, 0.745	0.677, 0.746	0.651, 0.746
Data completeness	0.998	0.996	0.999
θ (max)	26.739	27.108	27.111
$R_{reflections}$	0.0375(5329)	0.0386(4472)	0.0415(5201)
$wR^2_{reflections}$	0.0923(6266)	0.0997(5301)	0.1079(6322)
S	1.034	1.031	1.020
N_{par}	397	325	397

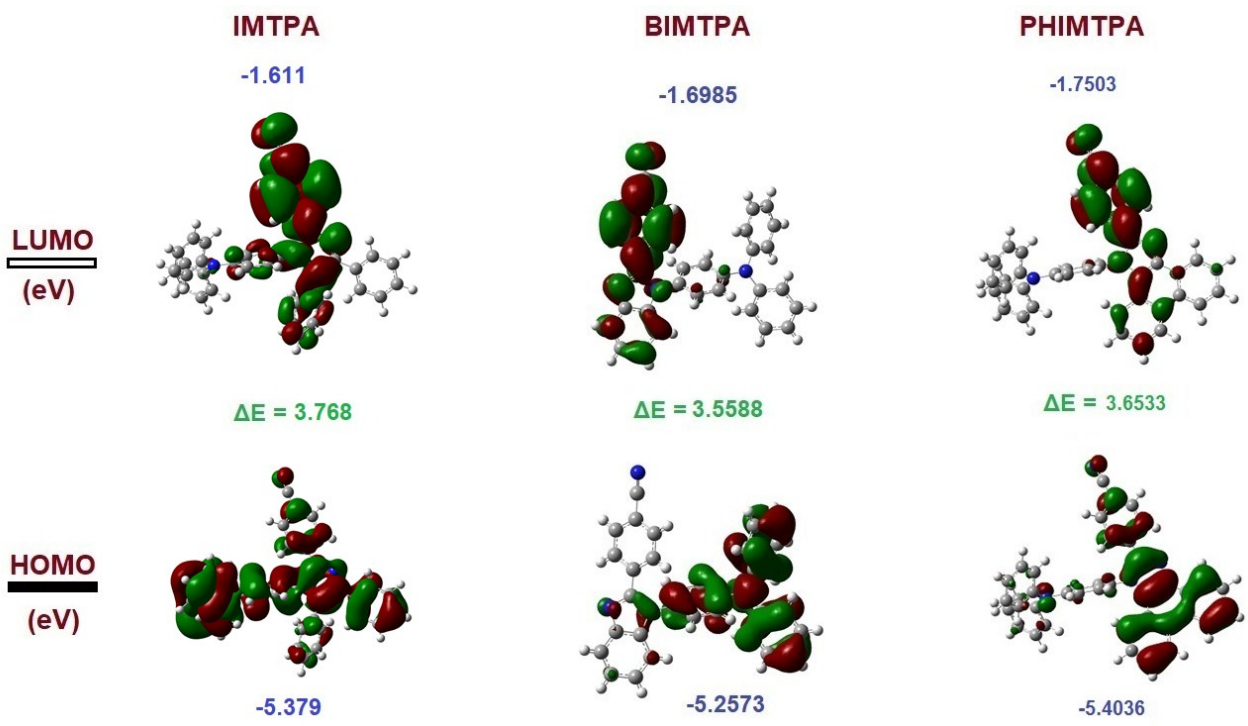

Fig. S1 Calculated HOMO-LUMO energy of **IMTPA**, **BIMTPA**, **PHIMTPA** and electron distribution on them in free state based on DFT/B3LYP/6-31G** calculations

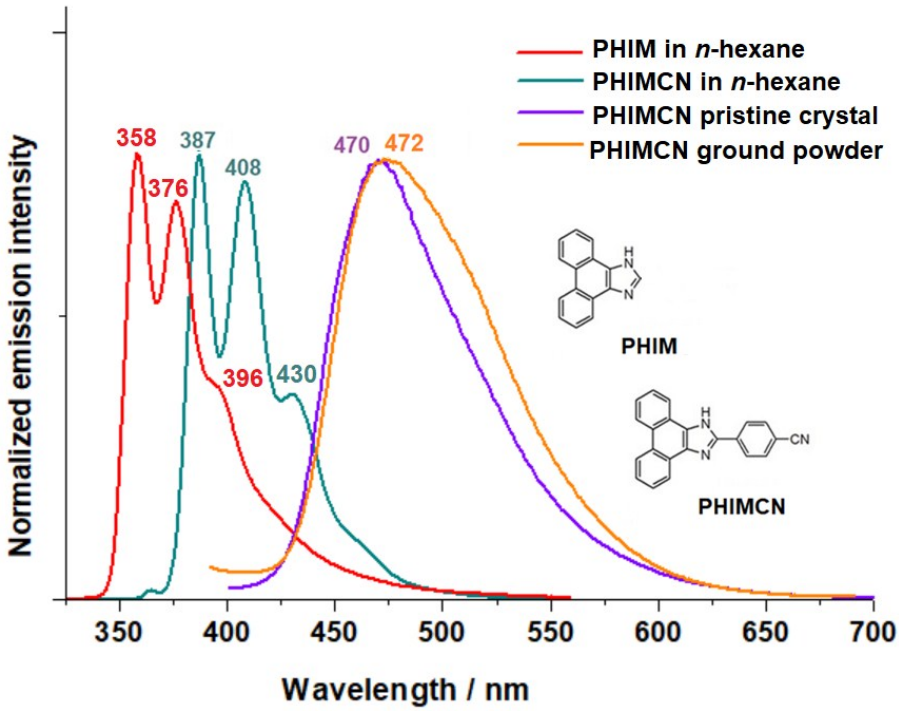

Fig. S2 Emission spectra of **PHIM** and **PHIMCN** under different conditions

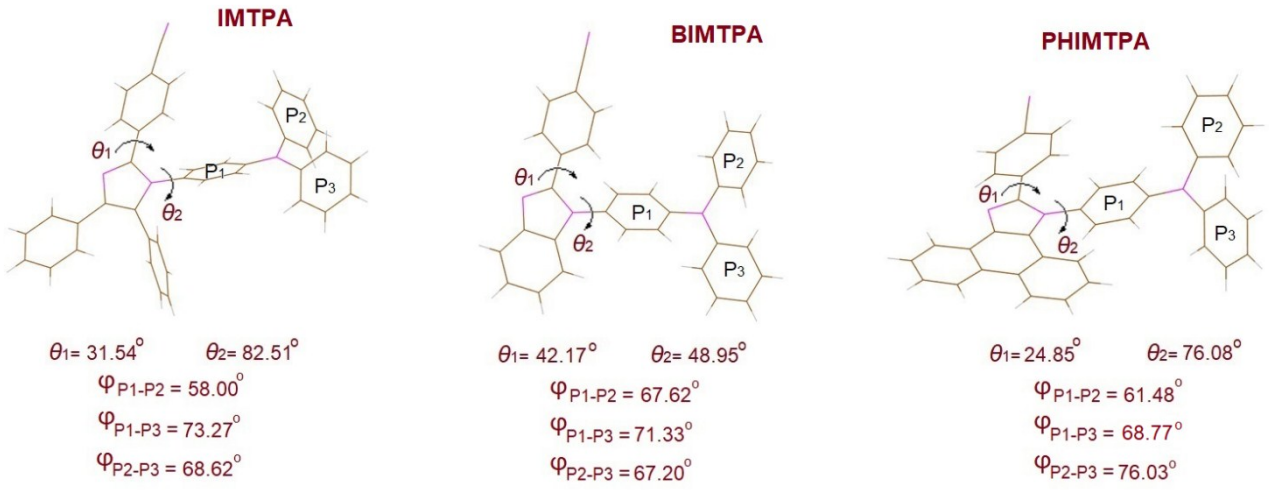

Fig. S3 Geometries of **IMTPA**, **BIMTPA** and **PHIMTPA** in crystalline phase

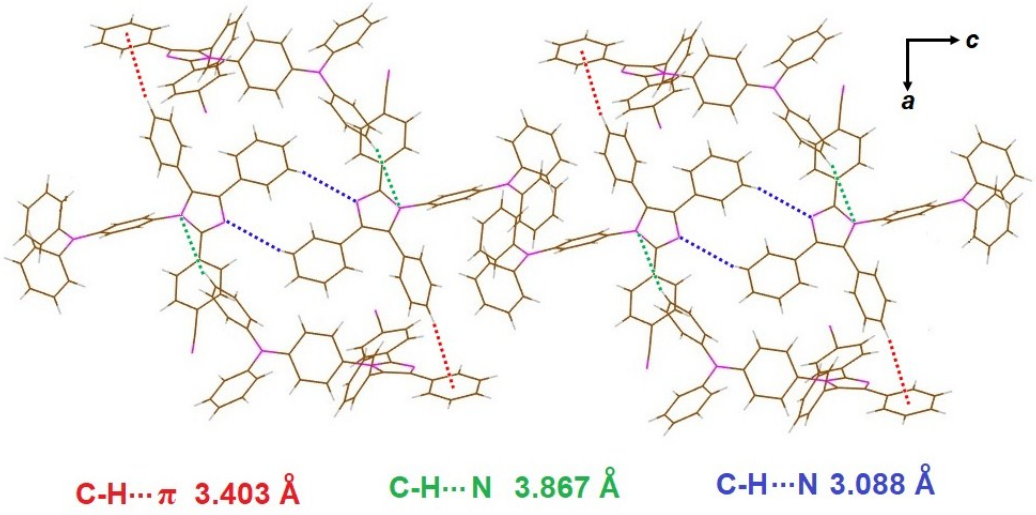

Fig. S4 molecular packing in **IMTPA** crystal

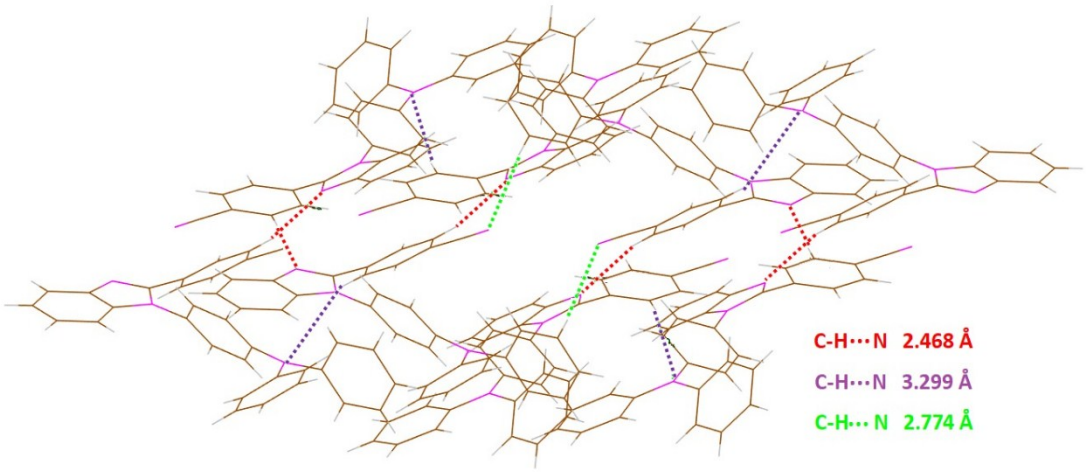

Fig. S5 molecular packing in **BIMTPA** crystal

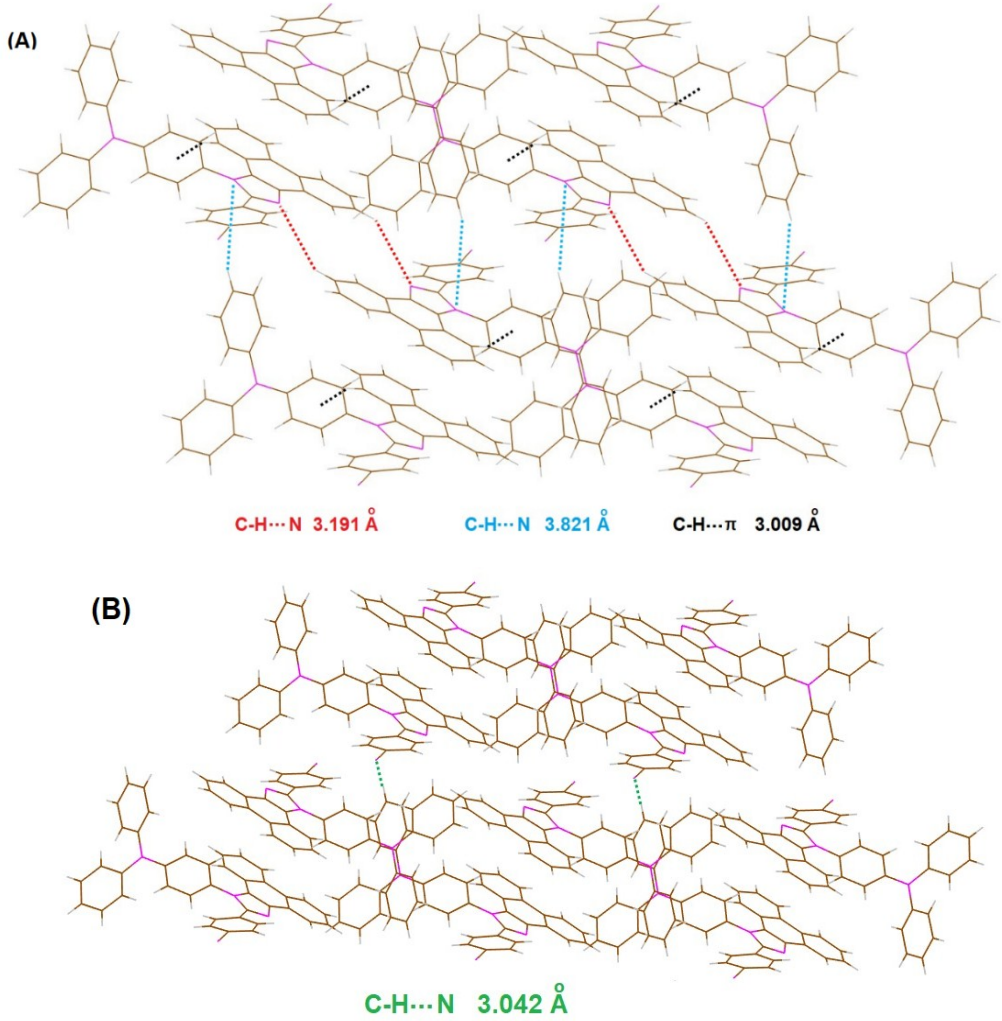

Fig. S6 molecular packing in **PHIMTPA** crystal

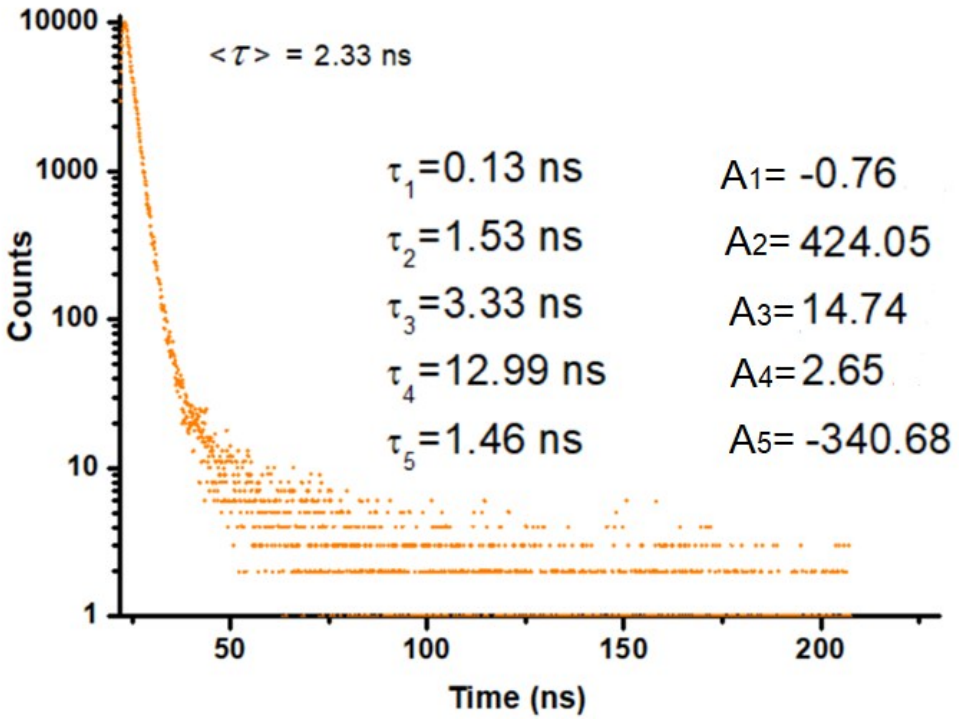

Fig. S7 Emission decay spectrum of **PHIMTPA** at 450 nm in as-prepared state

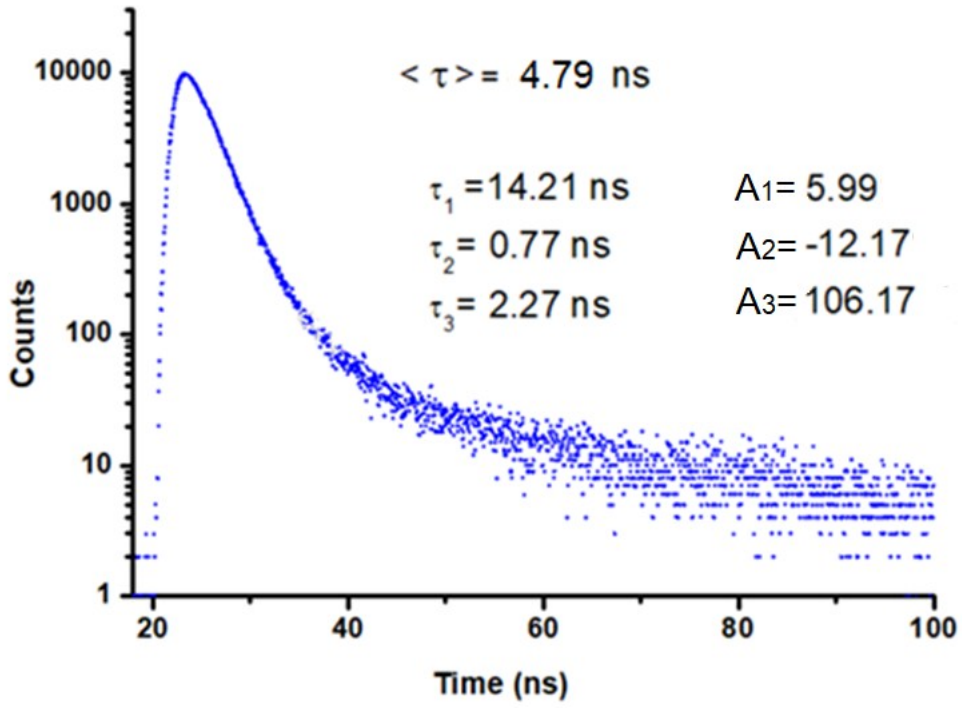

Fig. S8 Emission decay spectrum of **PHIMTPA** at 514 nm in as-prepared state

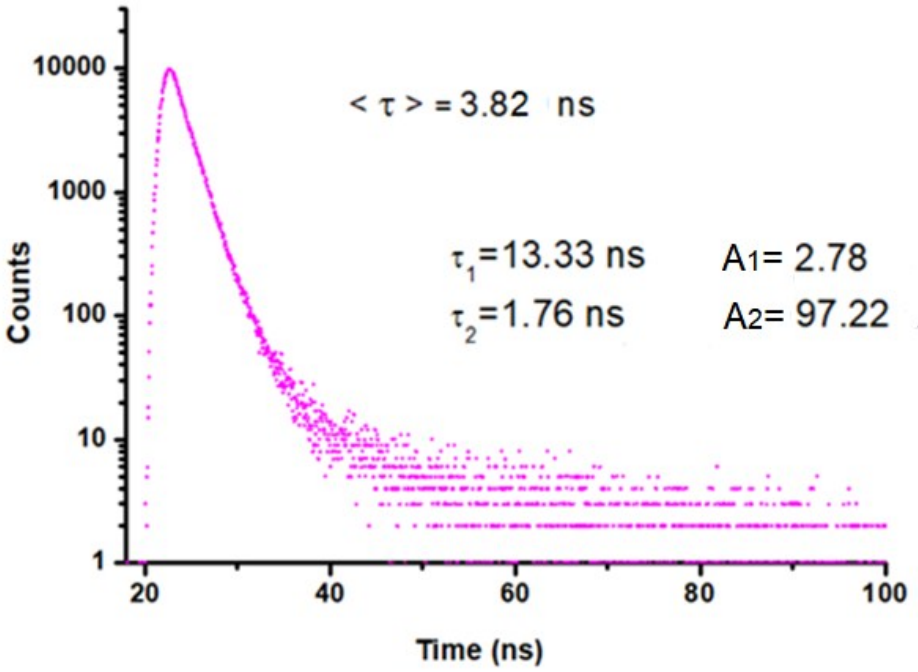

Fig. S9 Emission decay spectrum of **PHIMTPA** at 428 nm in as-prepared state

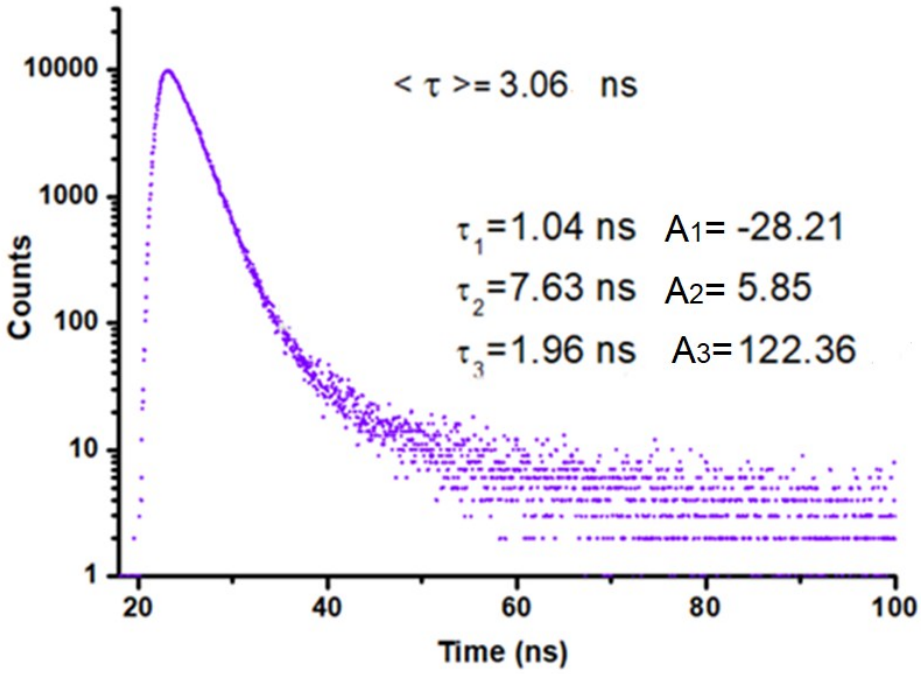

Fig. S10 Emission decay spectrum of **PHIMTPA** at 478 nm in as-prepared state

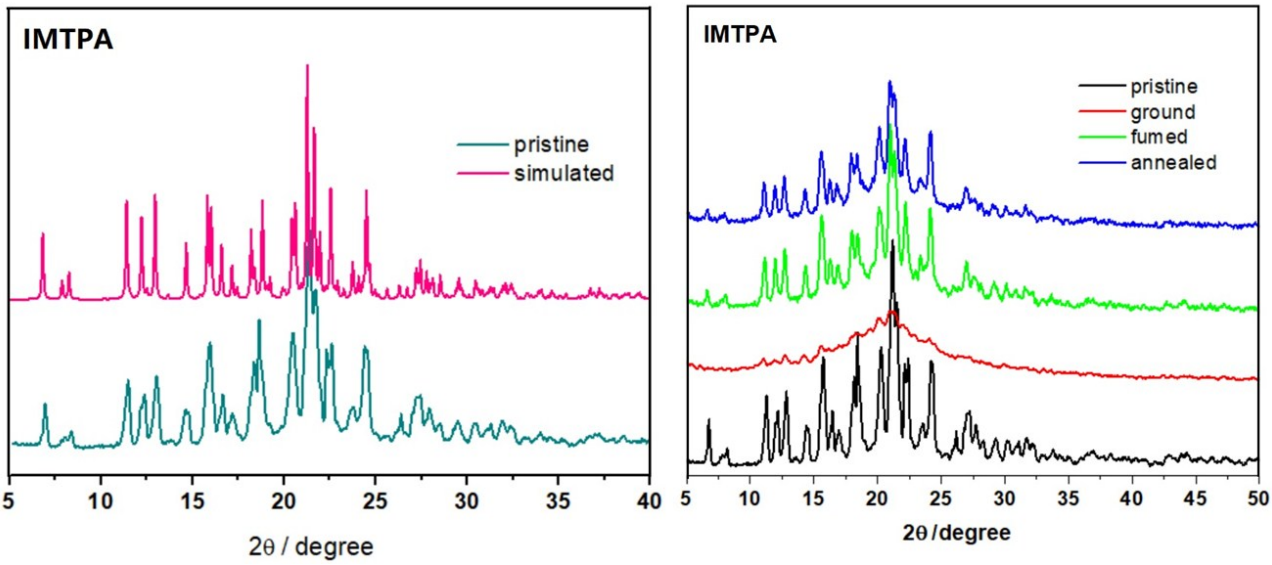

Fig. S11 Measured and simulated PXRD patterns of **IMTPA** (left); PXRD patterns of **IMTPA** under different conditions (right)

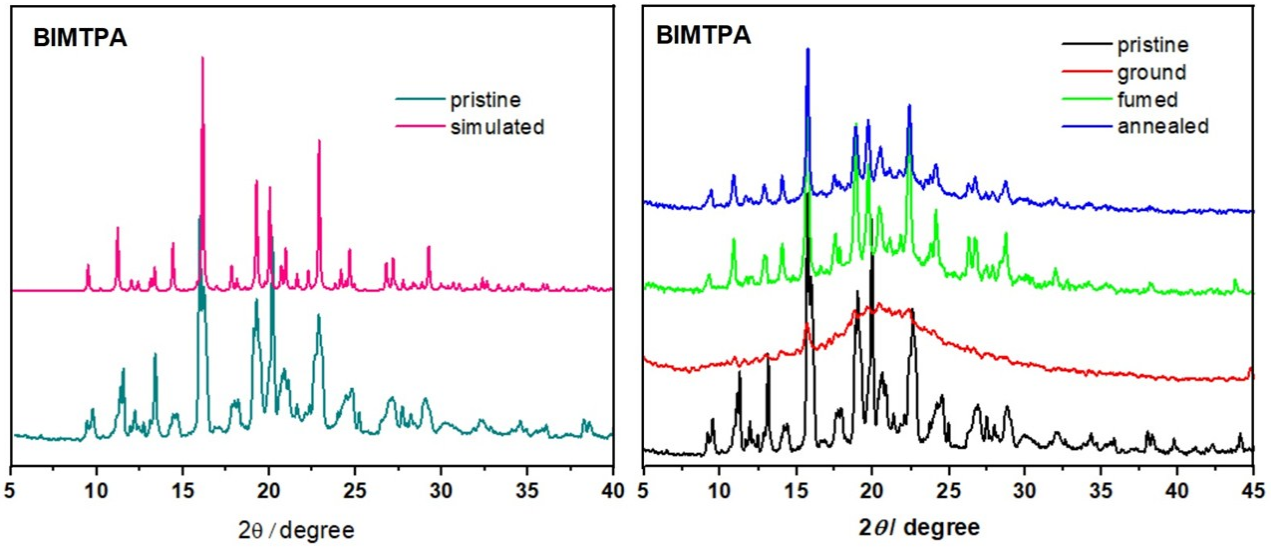

Fig. S12 Measured and simulated PXRD patterns of **BIMTPA** (left); PXRD patterns of **BIMTPA** under different conditions (right)

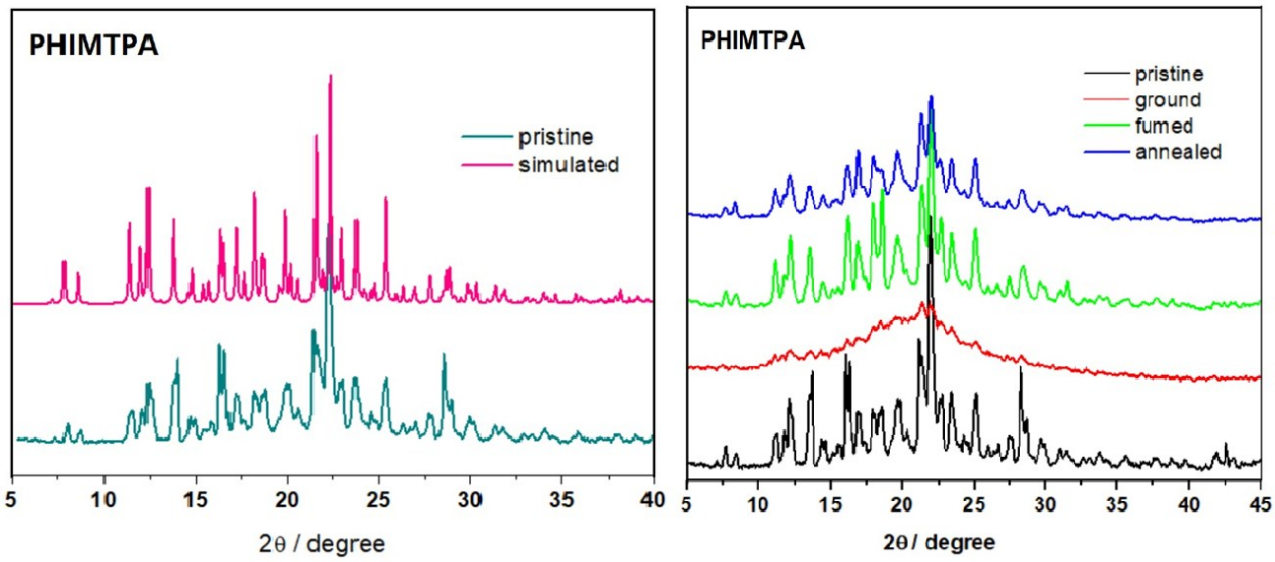

Fig. S13 Measured and simulated PXRD patterns of **PHIMTPA** (left); PXRD patterns of **PHIMTPA** under different conditions (right)

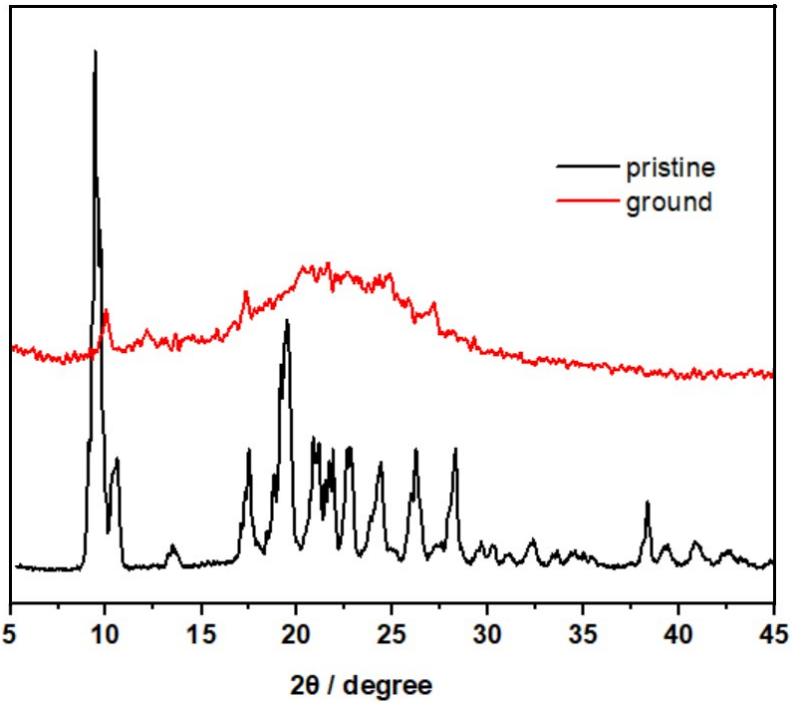

Fig. S14 PXRD patterns of **PHIMCN** under different conditions

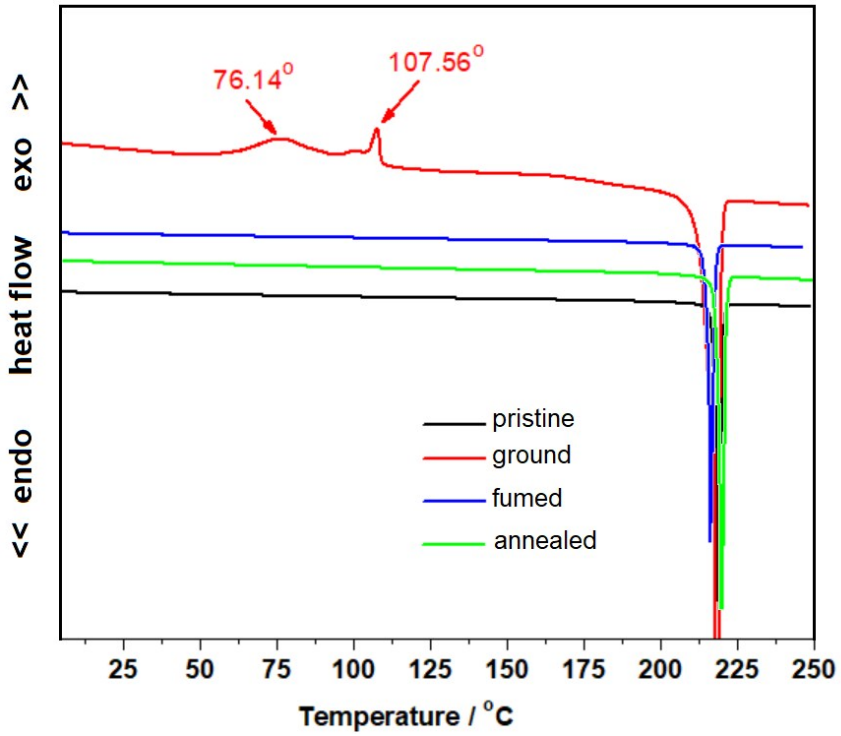

Fig. S15 DSC curves of **BIMTPA** under different conditions

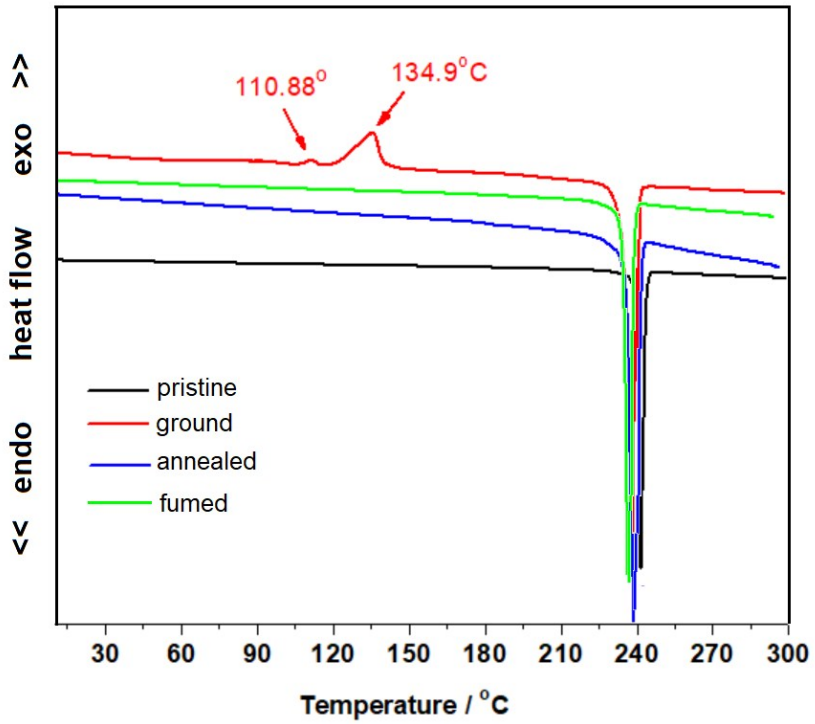

Fig. S16 DSC curves of **PHIMTPA** under different conditions

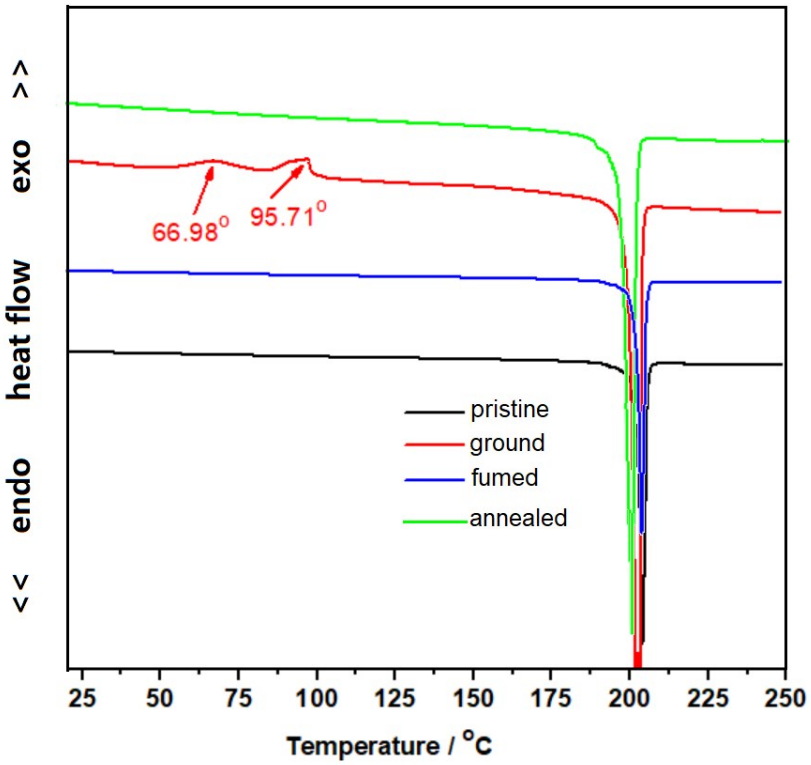

Fig. S17 DSC curves of **IMTPA** under different conditions

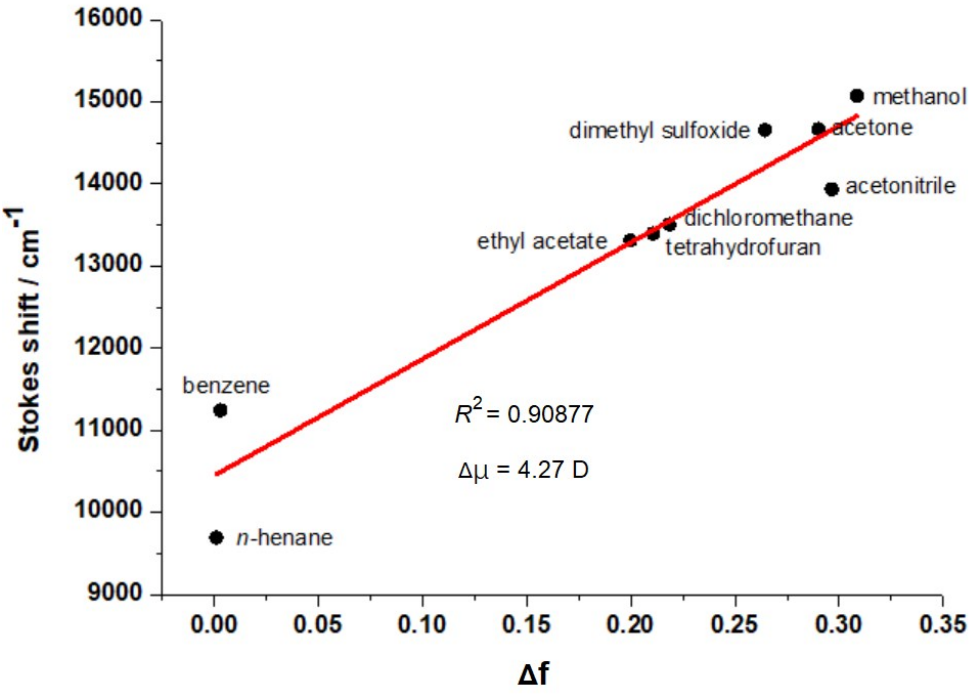

Fig. S18 Lippert-Mataga plot of **BIMTPA** in different solvents

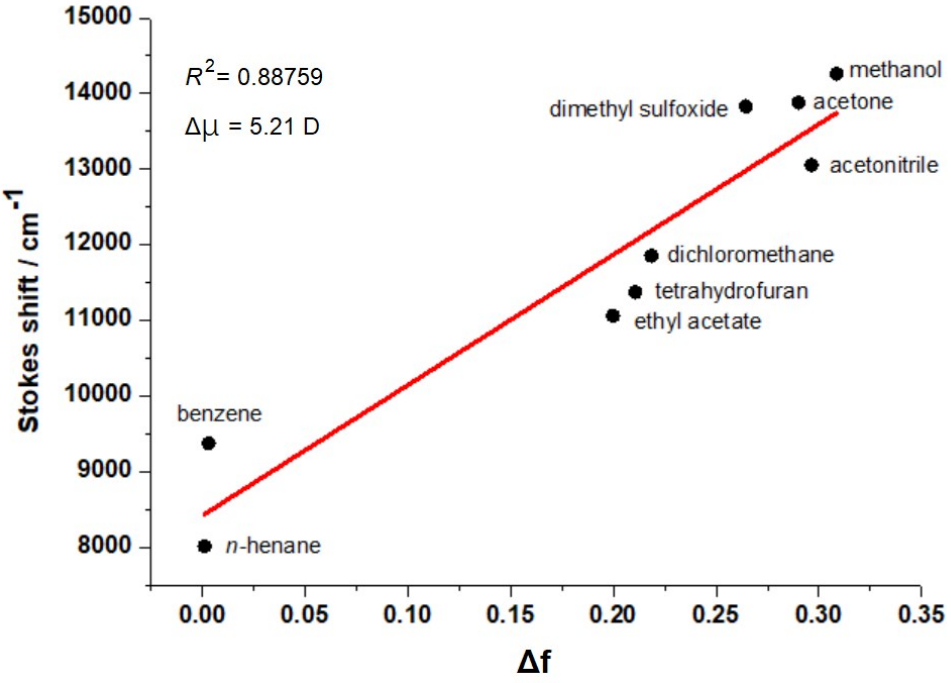

Fig. S19 Lippert-Mataga plot of **IMTPA** in different solvents

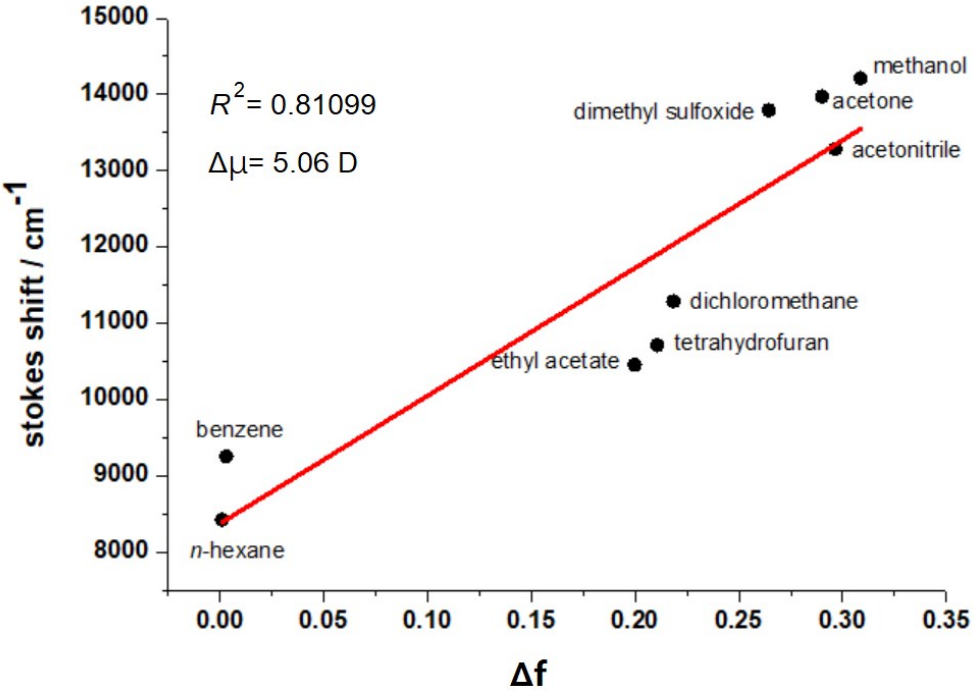

Fig. S20 Lippert-Mataga plot of **PHIMTPA** in different solvents

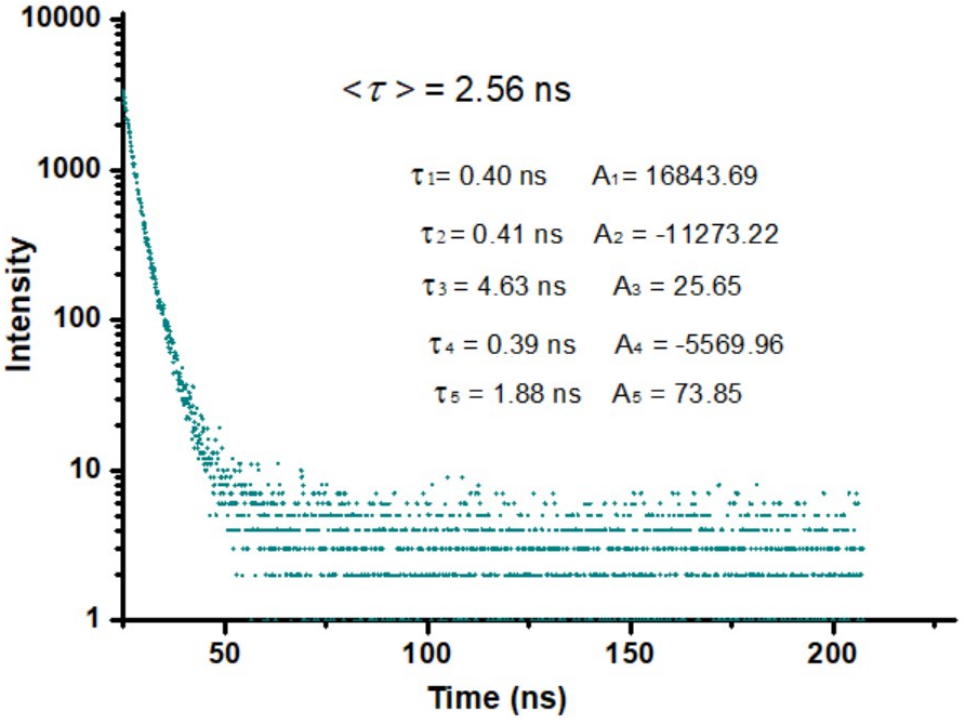

Fig. S21 Emission decay spectrum of **IMTPA** at 410 nm in as-prepared state

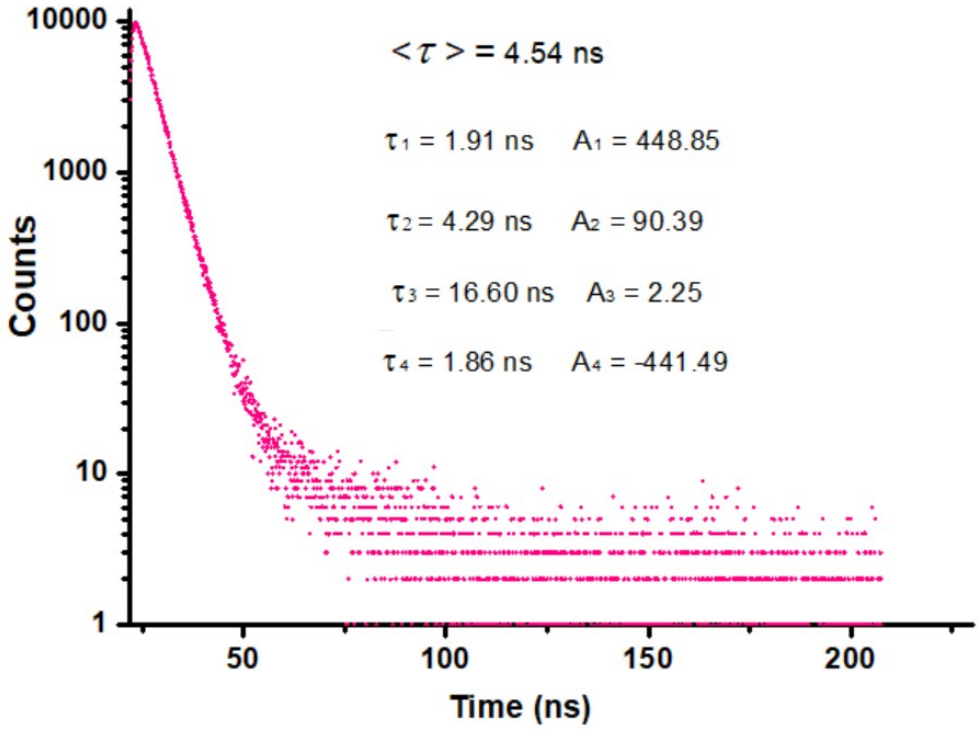

Fig. S22 Emission decay spectrum of **BIMTPA** at 435 nm in as-prepared state

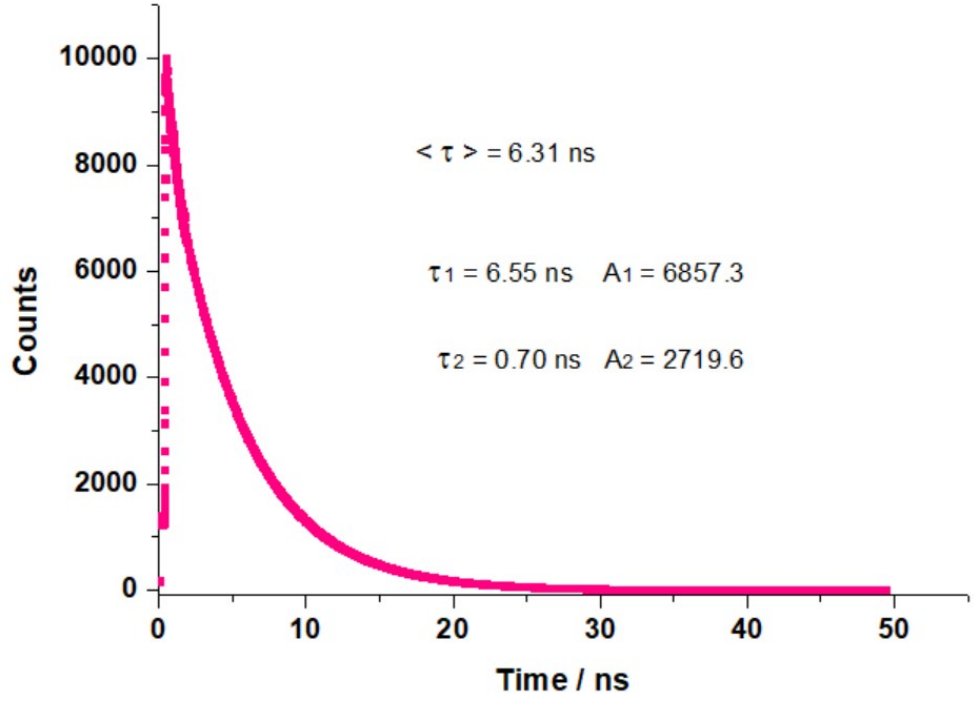

Fig. S23 Emission decay spectrum of **BIMTPA** at 467 nm in ground state

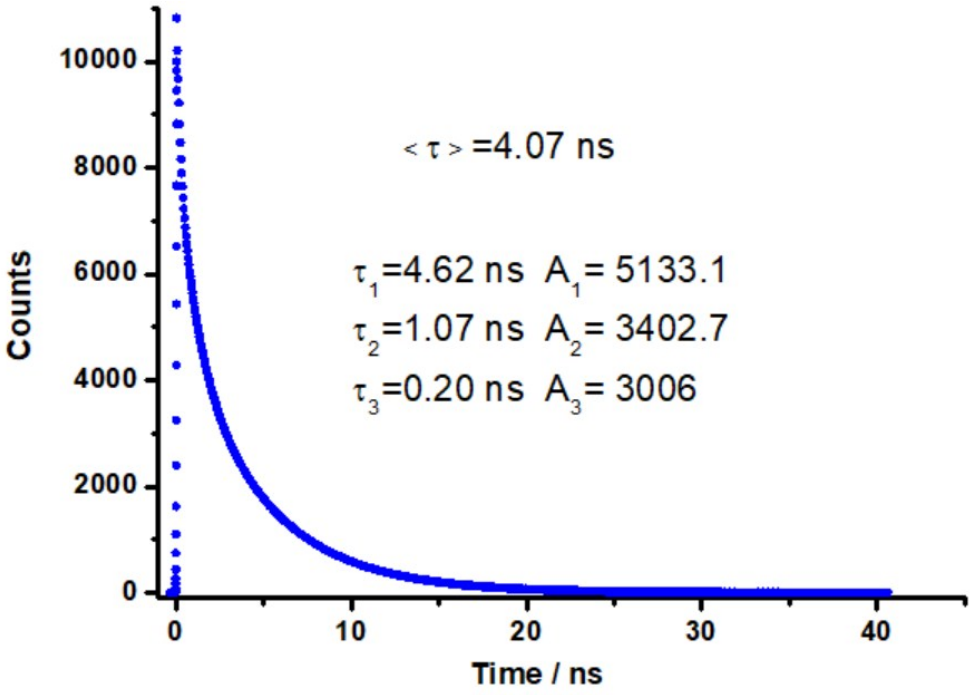

Fig. S24 Emission decay spectrum of **IMTPA** at 436 nm in ground state

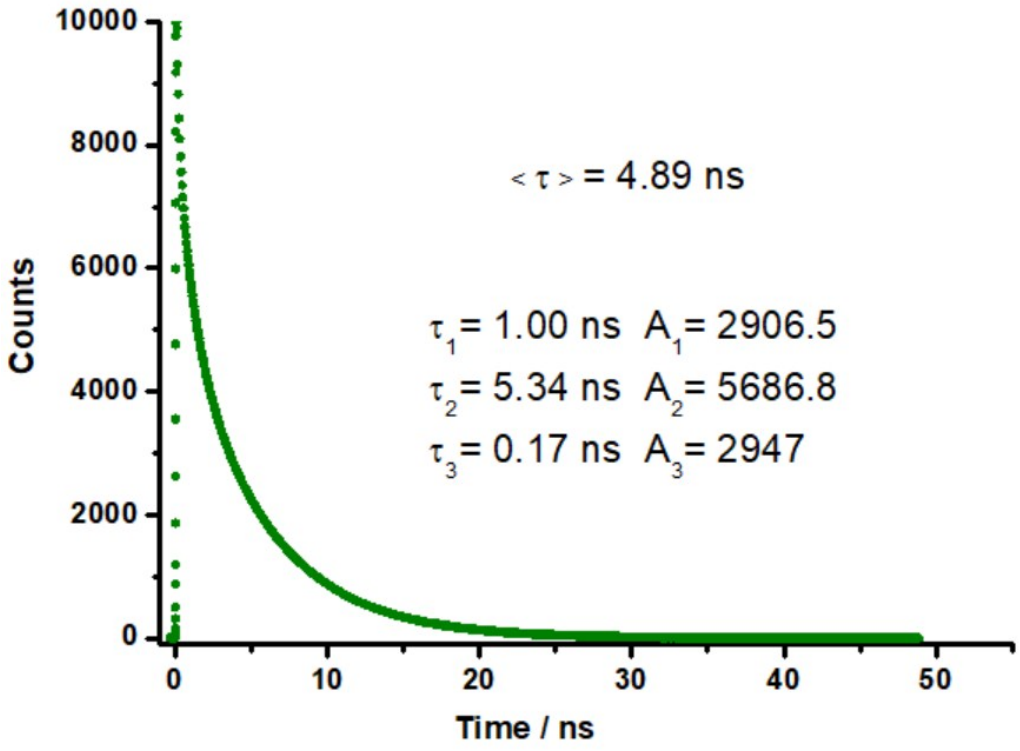

Fig. S25 Emission decay spectrum of **PHIMTPA** at 450 nm in ground state

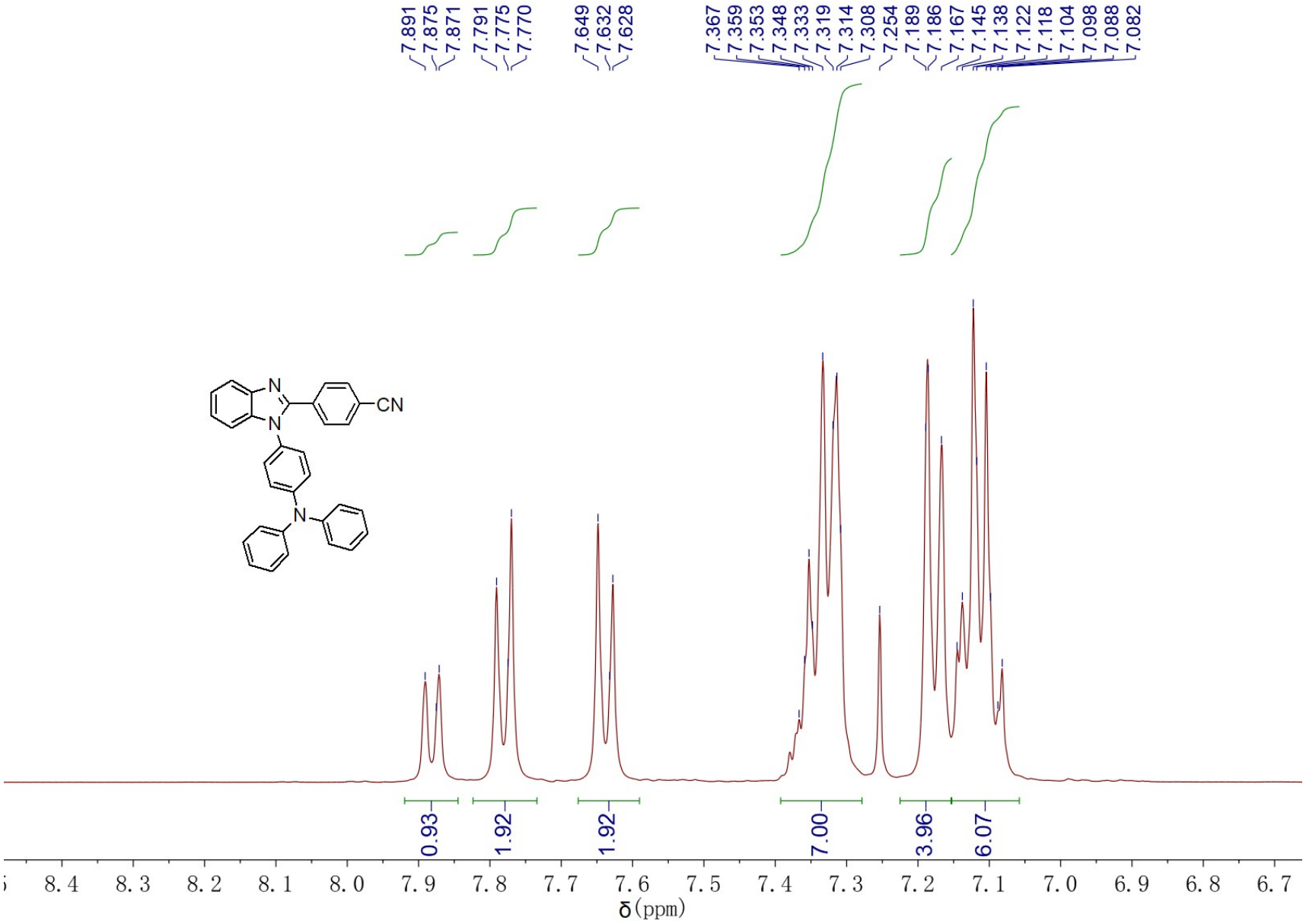
7.891
7.875
7.871
7.791
7.775
7.770
7.649
7.632
7.628
7.367
7.359
7.353
7.348
7.333
7.319
7.314
7.308
7.254
7.189
7.186
7.167
7.145
7.138
7.122
7.118
7.104
7.098
7.088
7.082
N
N
CN
N
0.93
1.92
1.92
7.00
3.96
6.07
8.4
8.3
8.2
8.1
8.0
7.9
7.8
7.7
7.6
7.5
7.4
7.3
7.2
7.1
7.0
6.9
6.8
6.7
δ(ppm)

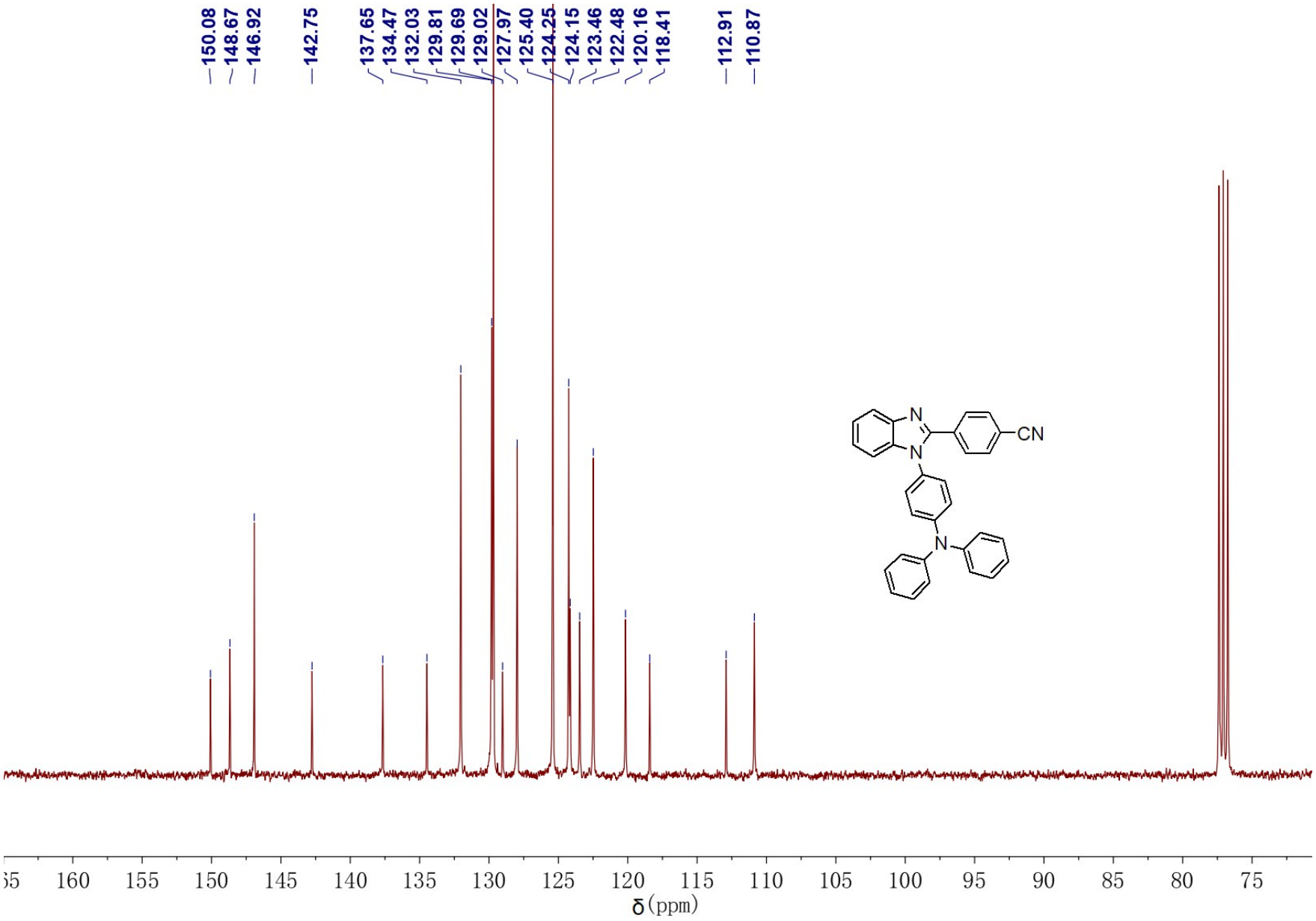
150.08
148.67
146.92
142.75
137.65
134.47
132.03
129.81
129.69
129.02
127.97
125.40
124.25
124.15
123.46
122.48
120.16
118.41
112.91
110.87
N
N
CN
N
160
155
150
145
140
135
130
125
120
115
110
105
100
95
90
85
80
75
δ(ppm)

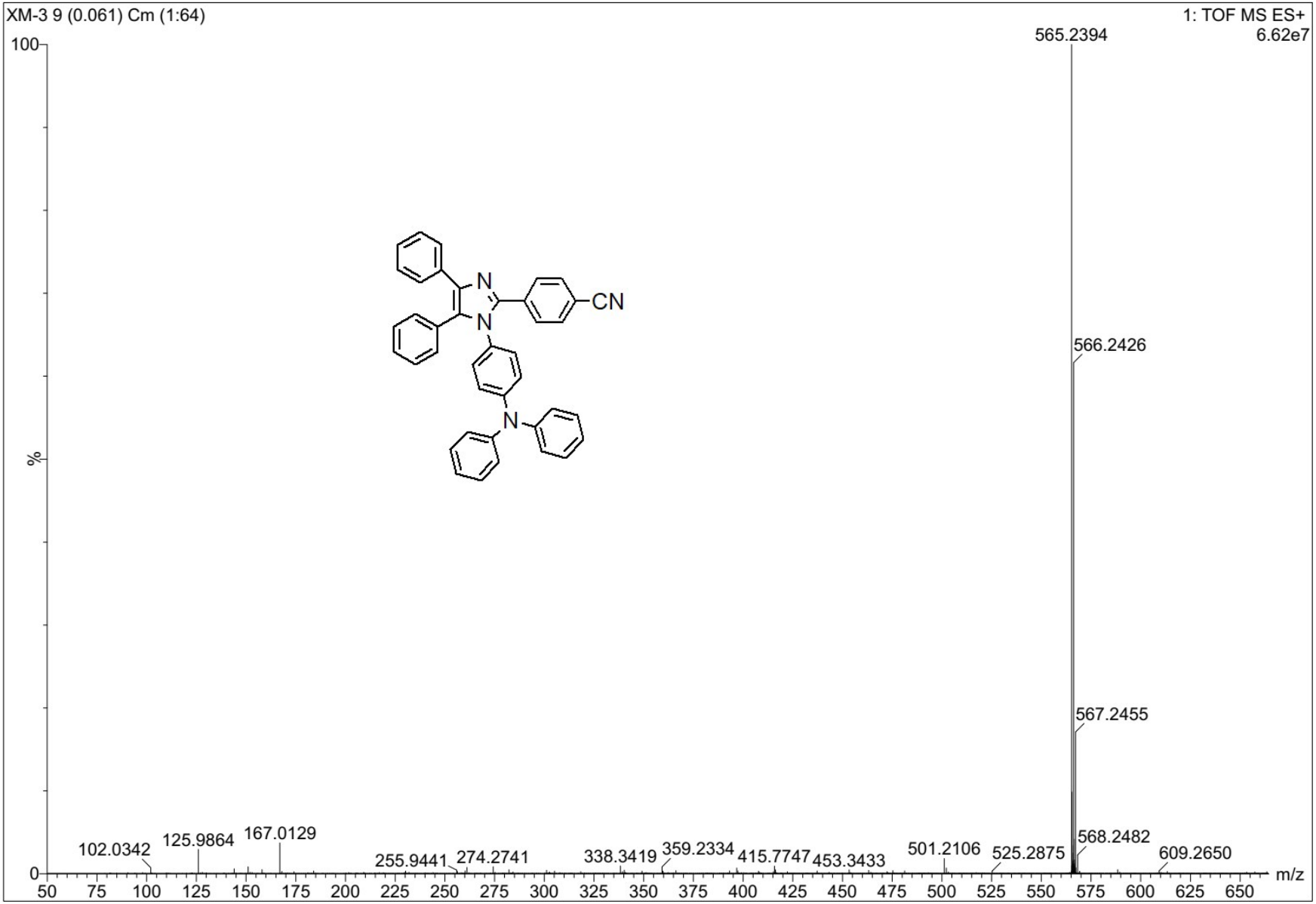
XM-3 9 (0.061) Cm (1:64)
1: TOF MS ES+
6.62e7
100
%
0
565.2394
566.2426
567.2455
568.2482
102.0342
125.9864
167.0129
255.9441
274.2741
338.3419
359.2334
415.7747
453.3433
501.2106
525.2875
609.2650
m/z
50 75 100 125 150 175 200 225 250 275 300 325 350 375 400 425 450 475 500 525 550 575 600 625 650
N
N
CN
N

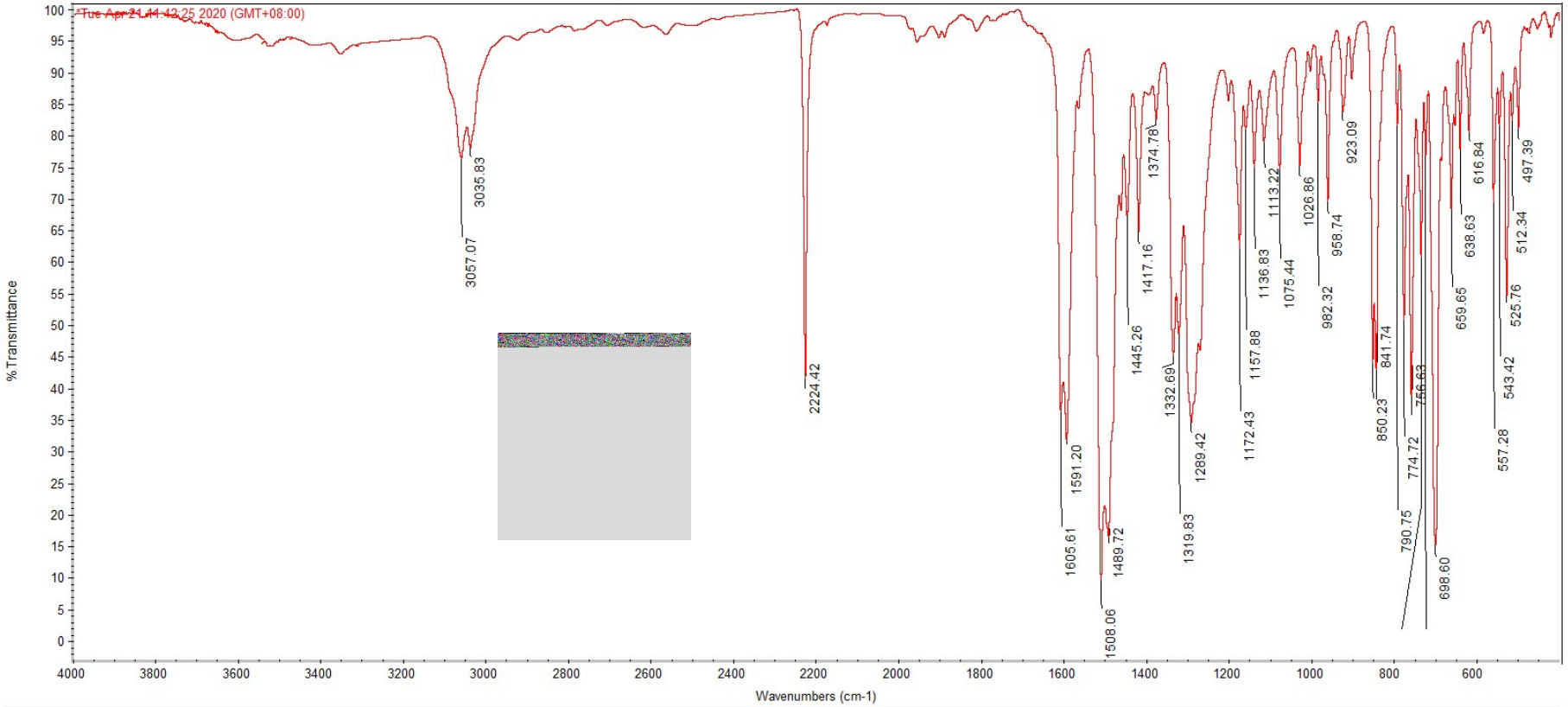
Tue Apr 21 14:42:25 2020 (GMT+08:00)
% Transmittance
Wavenumbers (cm-1)
3057.07
3035.83
2224.42
1605.61
1591.20
1508.06
1489.72
1445.26
1417.16
1374.78
1332.69
1319.83
1289.42
1172.43
1157.88
1136.83
1113.22
1075.44
1026.86
982.32
958.74
923.09
850.23
841.74
790.75
774.72
756.63
698.60
659.65
638.63
616.84
557.28
543.42
525.76
512.34
497.39

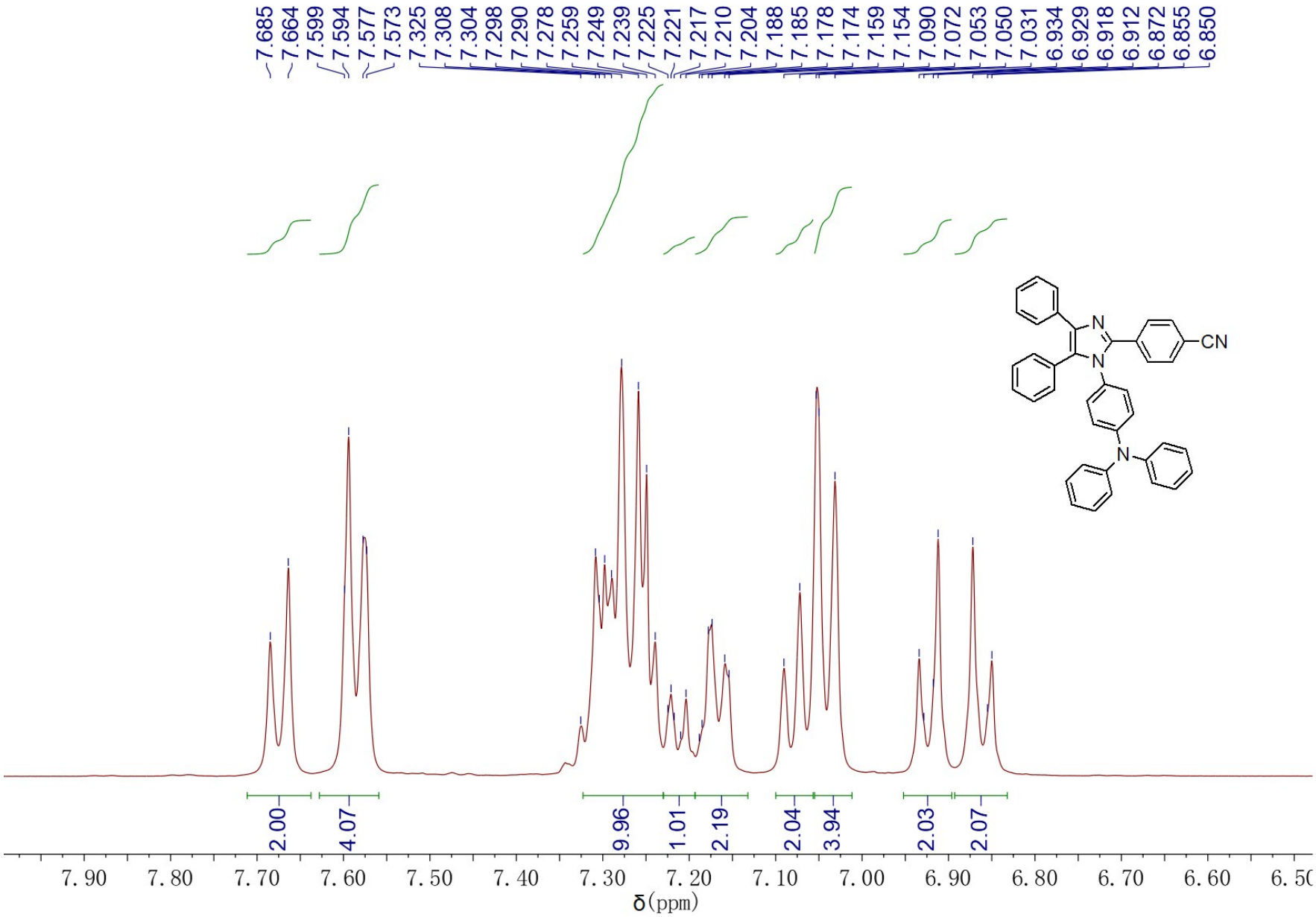
7.685
7.664
7.599
7.594
7.577
7.573
7.325
7.308
7.304
7.298
7.290
7.278
7.259
7.249
7.239
7.225
7.221
7.217
7.210
7.204
7.188
7.185
7.178
7.174
7.159
7.154
7.090
7.072
7.053
7.050
7.031
6.934
6.929
6.918
6.912
6.872
6.855
6.850
N
N
CN
N
2.00
4.07
9.96
1.01
2.19
2.04
3.94
2.03
2.07
7.90
7.80
7.70
7.60
7.50
7.40
7.30
7.20
7.10
7.00
6.90
6.80
6.70
6.60
δ(ppm)

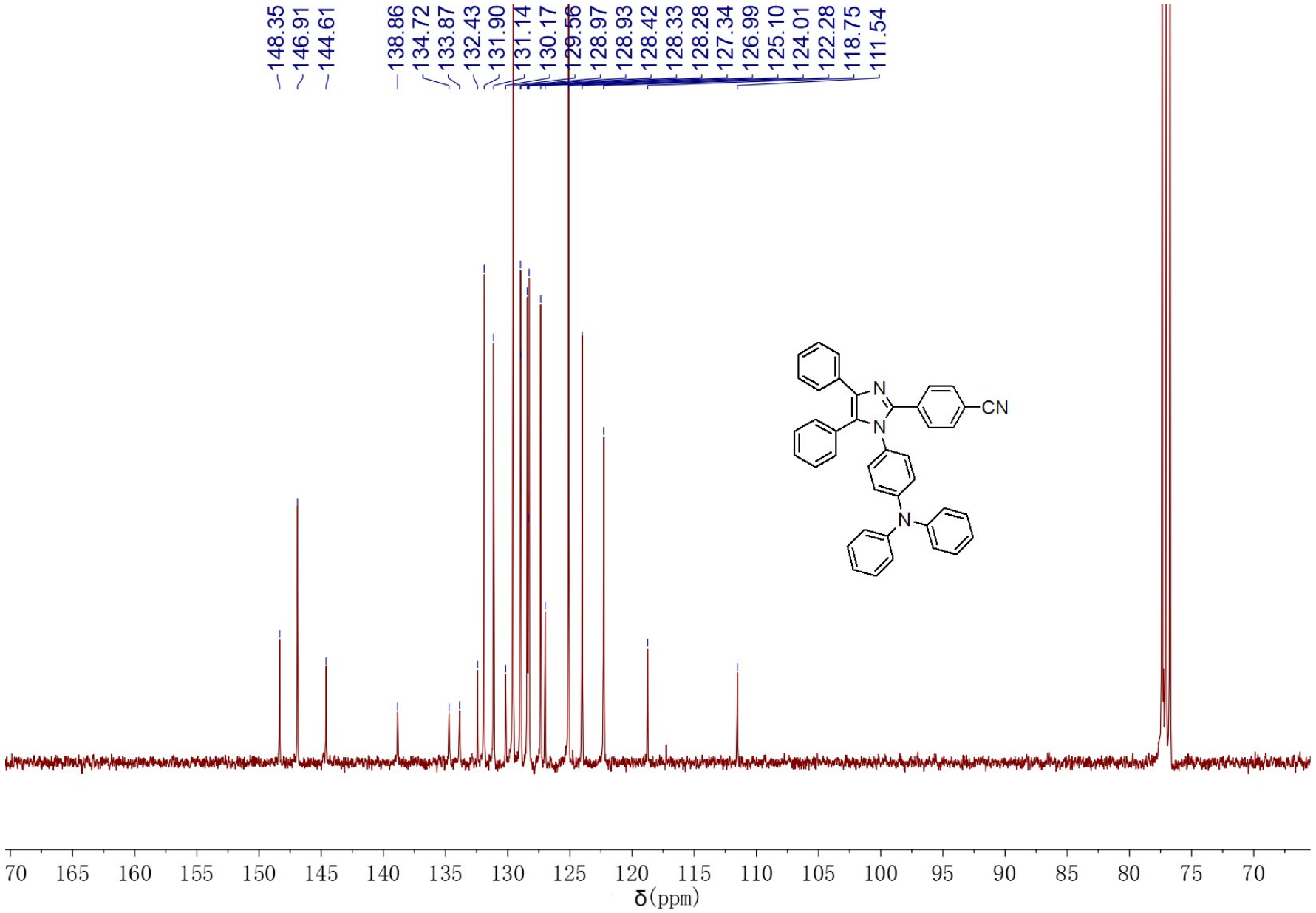
148.35
146.91
144.61
138.86
134.72
133.87
132.43
131.90
131.14
130.17
129.56
128.97
128.93
128.42
128.33
128.28
127.34
126.99
125.10
124.01
122.28
118.75
111.54
N
N
CN
N
70
165
160
155
150
145
140
135
130
125
120
115
110
105
100
95
90
85
80
75
70
δ(ppm)

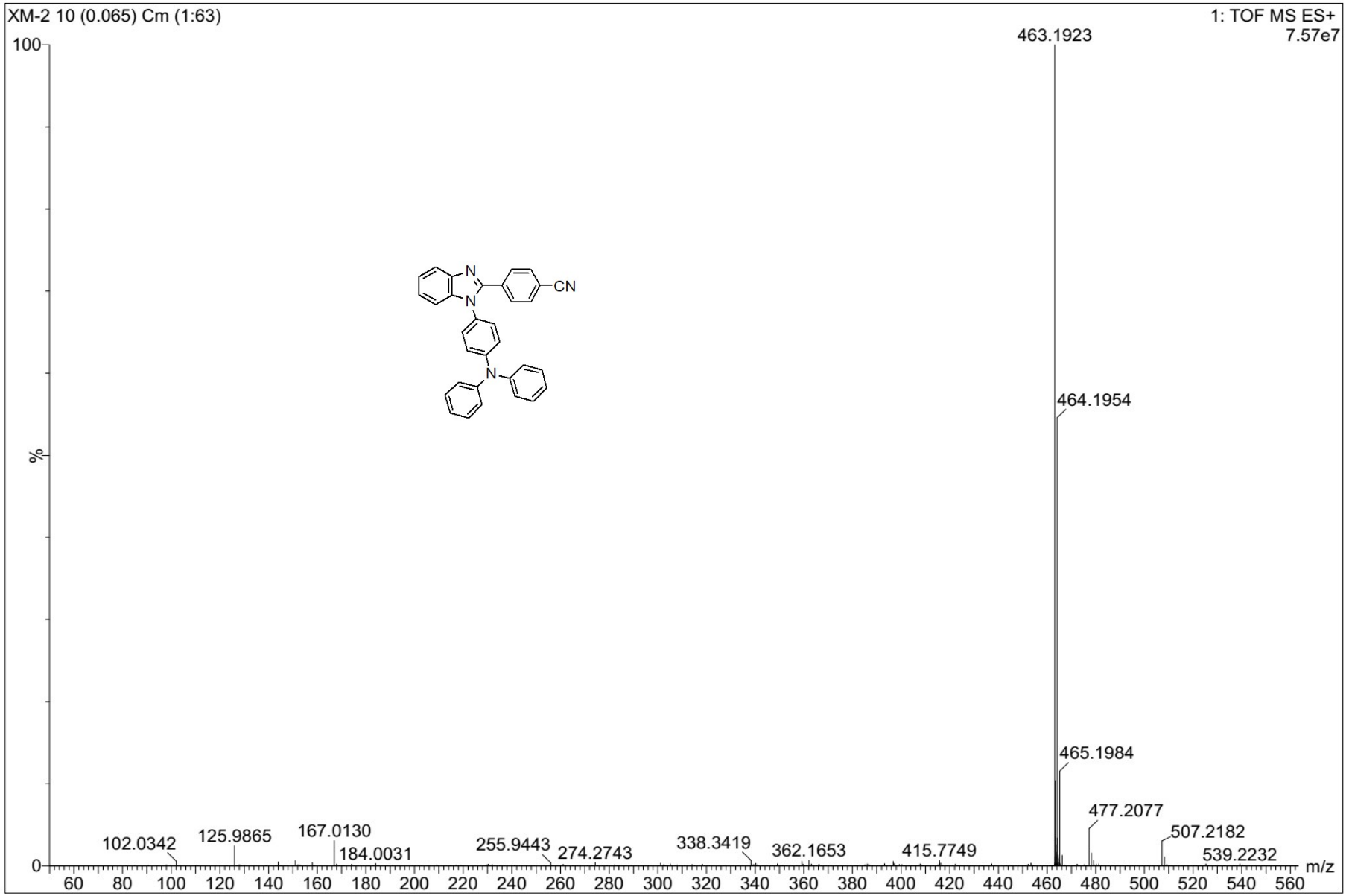
XM-2 10 (0.065) Cm (1:63)
1: TOF MS ES+
7.57e7
100
%
0
463.1923
464.1954
465.1984
477.2077
507.2182
539.2232
102.0342
125.9865
167.0130
184.0031
255.9443
274.2743
338.3419
362.1653
415.7749
N
N
CN
N
60 80 100 120 140 160 180 200 220 240 260 280 300 320 340 360 380 400 420 440 460 480 500 520 540 560
m/z

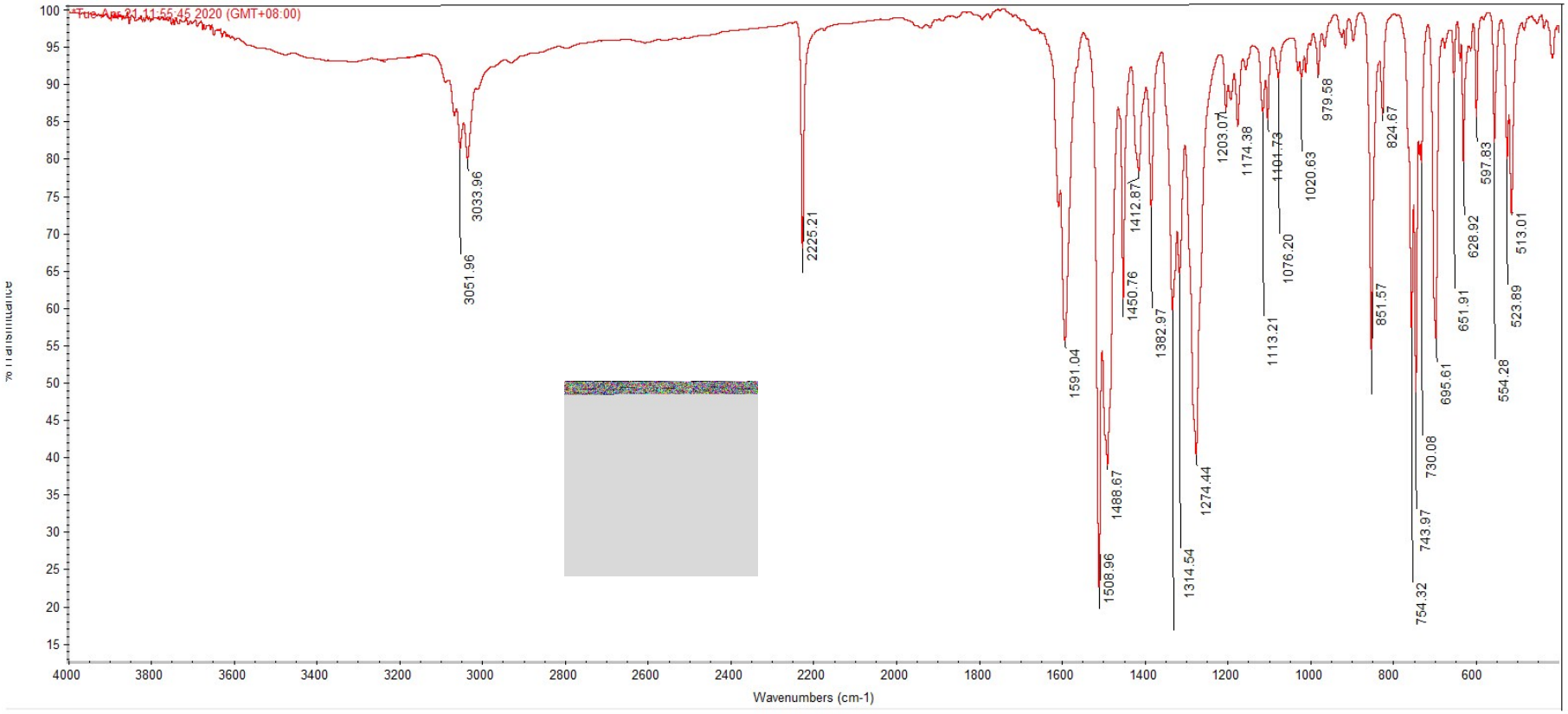
Tue Apr 21 11:55:45 2020 (GMT+08:00)
3051.96
3033.96
2225.21
1591.04
1508.96
1488.67
1450.76
1412.87
1382.97
1314.54
1274.44
1203.07
1174.38
1113.21
1101.73
1076.20
1020.63
979.58
851.57
824.67
754.32
743.97
730.08
695.61
651.91
628.92
597.83
554.28
523.89
513.01
Wavenumbers (cm-1)

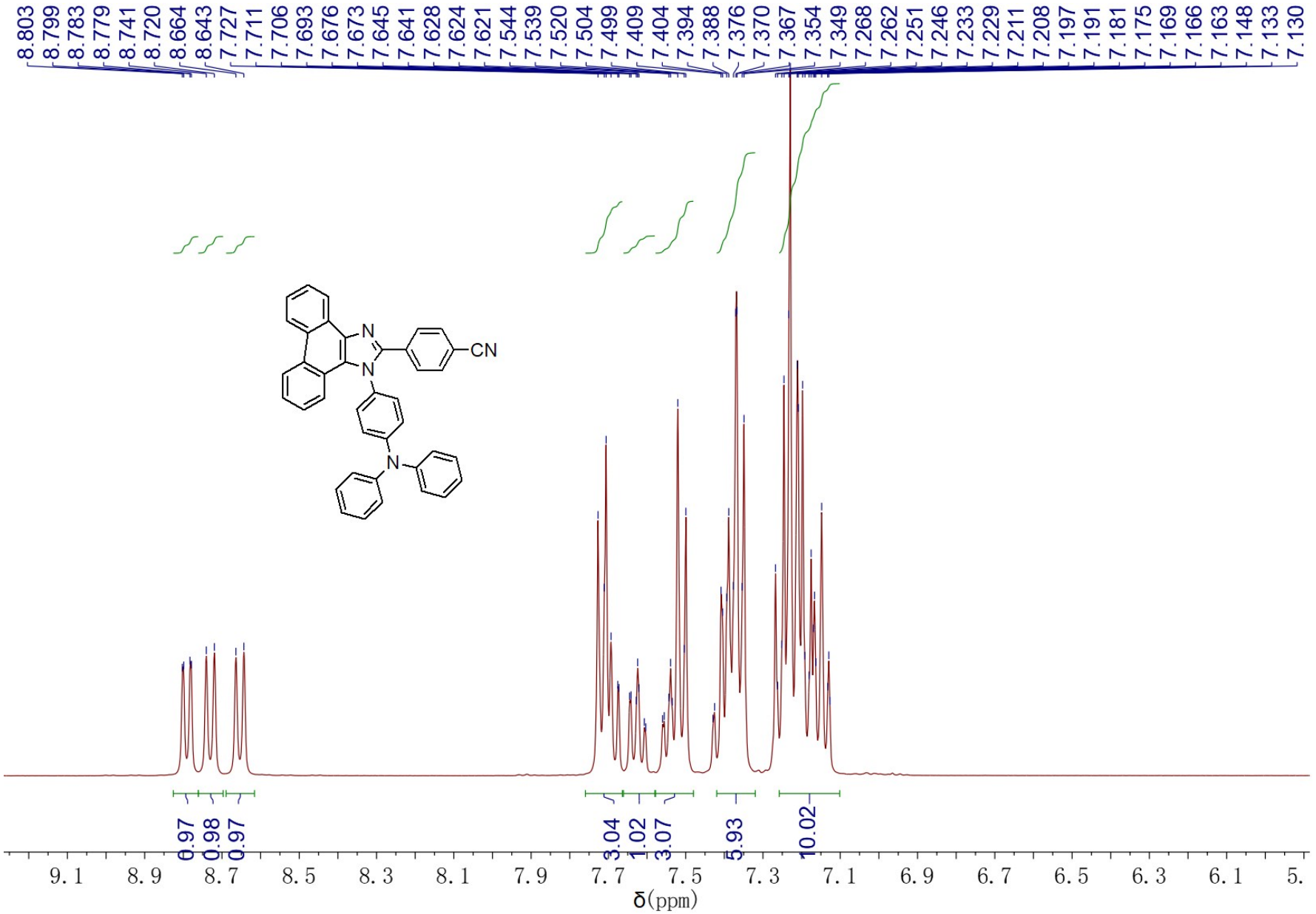
8.803
8.799
8.783
8.779
8.741
8.720
8.664
8.643
7.727
7.711
7.706
7.693
7.676
7.673
7.645
7.641
7.628
7.624
7.621
7.544
7.539
7.520
7.504
7.499
7.409
7.404
7.394
7.388
7.376
7.370
7.367
7.354
7.349
7.268
7.262
7.251
7.246
7.233
7.229
7.211
7.208
7.197
7.191
7.181
7.175
7.169
7.166
7.163
7.148
7.133
7.130
N
N
CN
N
0.97
0.98
0.97
3.04
1.02
3.07
5.93
10.02
9.1
8.9
8.7
8.5
8.3
8.1
7.9
7.7
7.5
7.3
7.1
6.9
6.7
6.5
6.3
6.1
5.
δ(ppm)

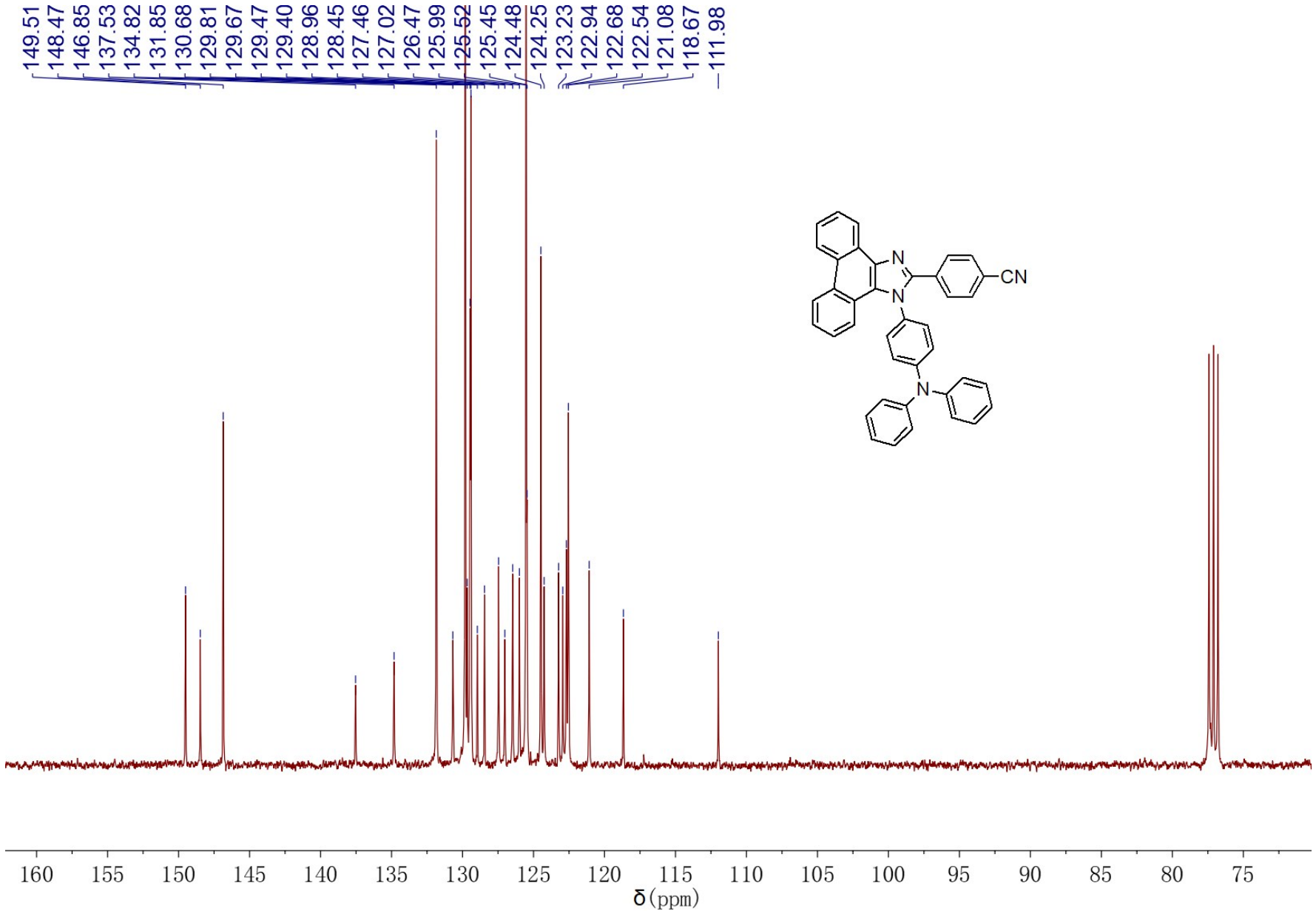
149.51
148.47
146.85
137.53
134.82
131.85
130.68
129.81
129.67
129.47
129.40
128.96
128.45
127.46
127.02
126.47
125.99
125.52
125.45
124.48
124.25
123.23
122.94
122.68
122.54
121.08
118.67
111.98
N
N
CN
N
160
155
150
145
140
135
130
125
120
115
110
105
100
95
90
85
80
75
δ(ppm)

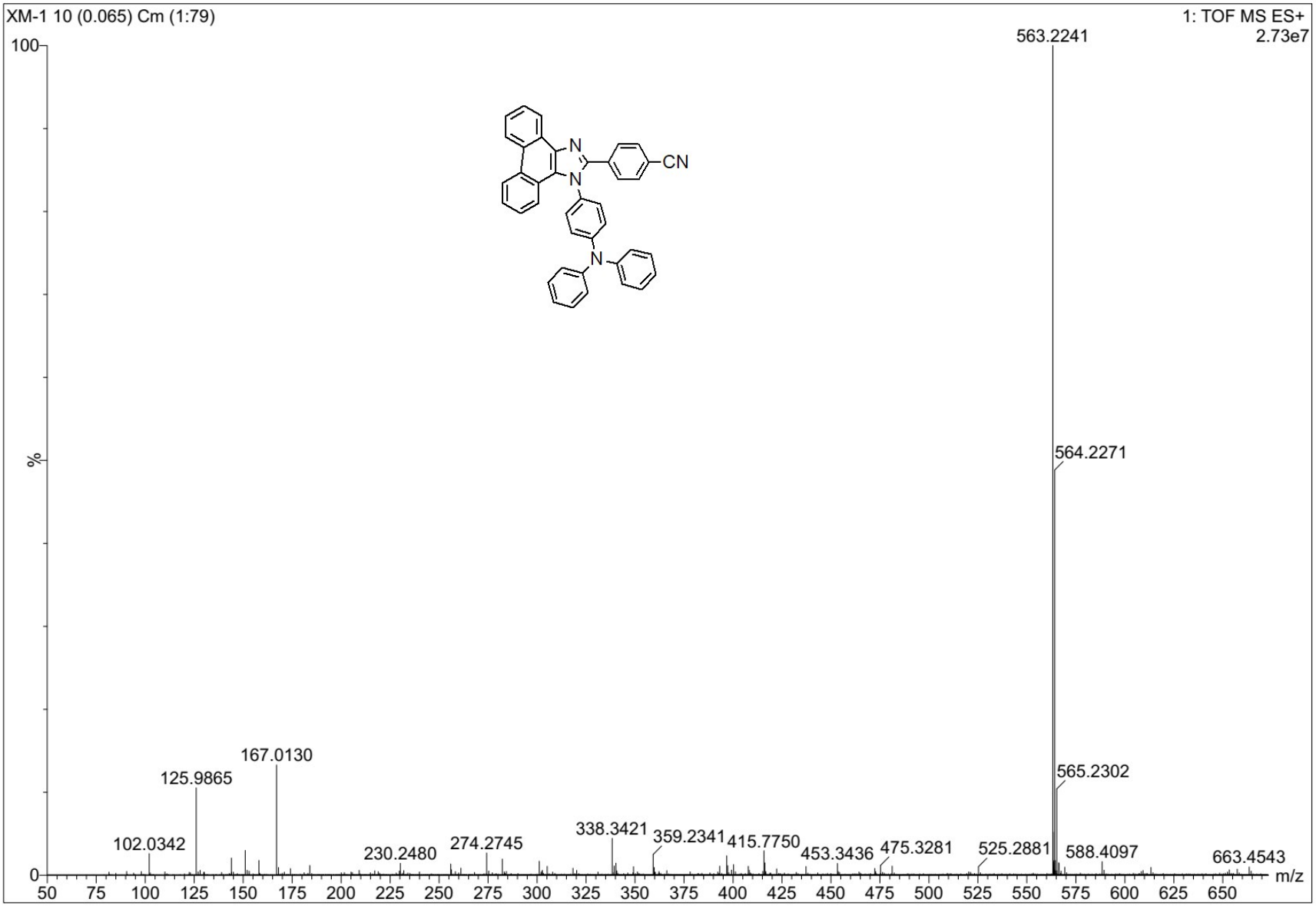
XM-1 10 (0.065) Cm (1:79)
1: TOF MS ES+
2.73e7
100
%
0
563.2241
564.2271
565.2302
167.0130
125.9865
102.0342
230.2480
274.2745
338.3421
359.2341
415.7750
453.3436
475.3281
525.2881
588.4097
663.4543
m/z
50 75 100 125 150 175 200 225 250 275 300 325 350 375 400 425 450 475 500 525 550 575 600 625 650
N
N
CN
N

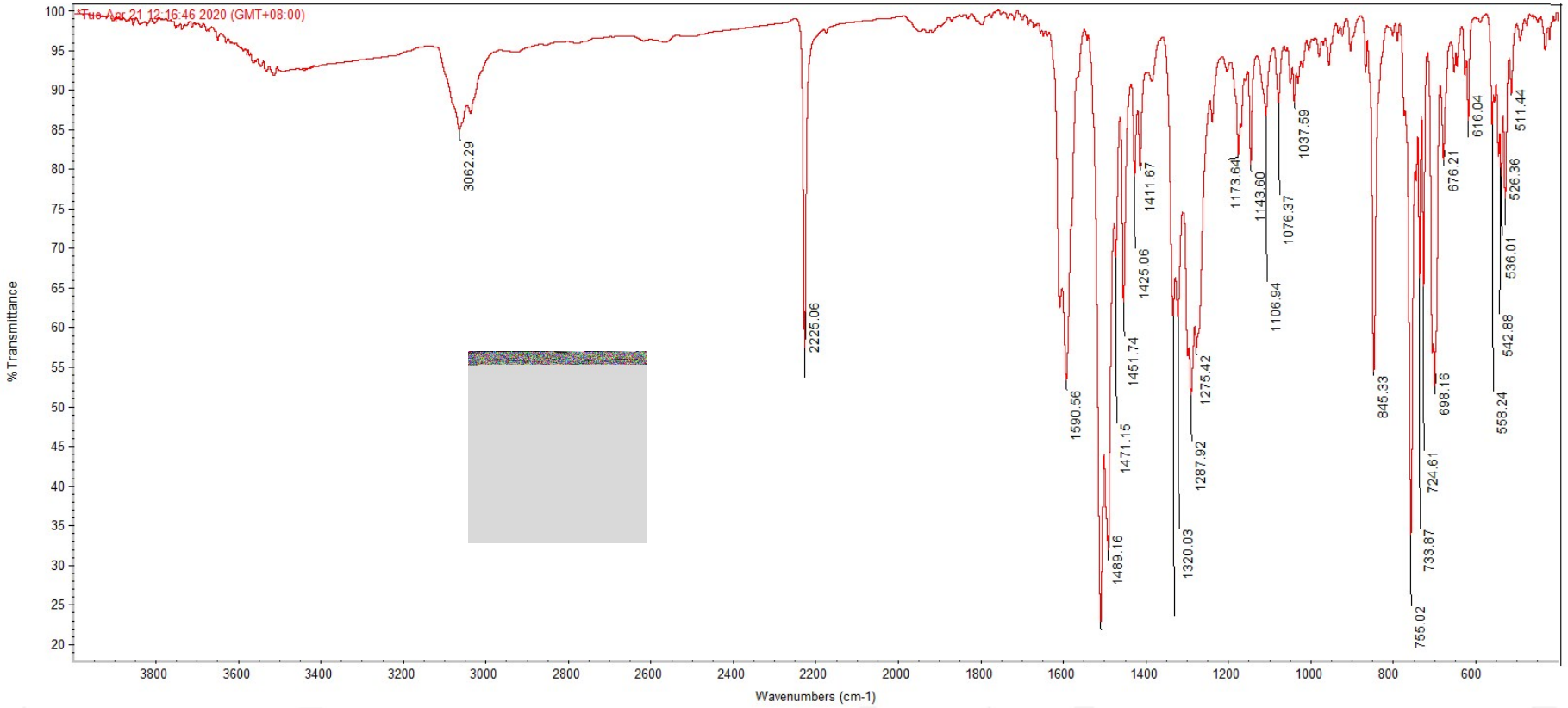
Tue Apr 21 12:16:46 2020 (GMT+08:00)
% Transmittance
Wavenumbers (cm-1)
3062.29
2225.06
1590.56
1489.16
1471.15
1451.74
1425.06
1411.67
1320.03
1287.92
1275.42
1173.64
1143.60
1106.94
1076.37
1037.59
845.33
755.02
733.87
724.61
698.16
676.21
616.04
558.24
542.88
536.01
526.36
511.44